

**LOAD TESTING OF WOOD-CONCRETE BEAMS INCORPORATING  
RECYCLED UTILITY POLES**

**Matthew R. LeBorgne**

**Richard M. Gutkowski**

**April 2008**

## **ABSTRACT**

A wood-concrete composite bridge constructed of recycled utility poles is a potentially cost effective solution to repair a portion of the 108,647 rural bridges that have been deemed functionally obsolete or structurally deficient and have a span under thirty feet in length. Wood-concrete bridges have been in use since 1929 with an excellent record of accomplishment for performance and durability with some bridges still in use after 69 years of service. This research project focuses on developing a design method for predicting the capacity of a composite longitudinal bridge deck section consisting of two utility poles topped with an interconnected concrete layer. The wood-concrete section is analyzed as a layered beam by using load and resistance factor design assuming the beam is fully composite. Adjustment factors are calculated to consider the additional mid-span stresses due to partially composite action. Full scale testing of the cast-in-place beams with a 29.52 ft span was performed with service and ultimate loads as high as 12.22 kips and 37.98 kips, respectively. The highest composite efficiency of the wood-concrete beams was determined to be 96.4 percent. An empirical relationship for modeling the time-dependent deflection during the critical 28-day curing period of the wood-concrete beams was developed.

“The contents of this report reflect the views of the authors, who are responsible for the facts and the accuracy of the information presented. This document is disseminated under the sponsorship of the Department of Transportation, University Transportation Centers Program, in the interest of information exchange. The U.S. Government assumes no liability for the contents or use thereof.”

## EXECUTIVE SUMMARY

Nationwide, many bridges are in a state of agedness, disrepair and/or structural or functional deficiency. In rural settings, county jurisdictions have numerous inventoried bridges in such condition but very limited funds for repair/replacement. Only a very small proportion can be addressed annually. Secondary roads and rural arterials are characterized by many short span bridges of 40 feet or less. Numerous bridges shorter than 20 feet long exist, especially over streams and ditches on agricultural land, or in state and national parks. Sub-20 foot bridges are not eligible for federal bridge infrastructure funds, so are frequently, if not commonly, neglected. Thus, innovative, low material cost short span bridges, which are readily built by unskilled labor, are a boon to small rural jurisdictions and on park lands.

This project involved conceiving and configuring a composite bridge comprised of concrete and wood utility poles. The concept was to use utility poles as either stringers or a solid deck beneath a conventional reinforced concrete bridge deck. Frequently, wood utility poles are replaced as part of secondary road reconstruction, such as widening roadways. Many of the removed poles are still sound structurally and usable. Instead of discarding these members it was worthwhile to investigate viable alternatives uses. Since utility poles are commonly 30-60 feet long, sometimes longer, they can be a low cost recycled resource for short and medium span bridge construction. Indeed, the PI readily accomplished a donation of the utility poles from the utility company for use, suggesting a possible future low cost or no cost material source.

The concept of a longitudinal deck bridge comprised of a solid layer of utility poles, i.e., several poles side by side, topped by an interconnected concrete layer was conceived. A high degree of composite action of the layered system was anticipated from the notched shear key anchor used for interlayer connection. Natural taper of the members was used to create desired camber. A design procedure based on conventional mechanics analysis and an assumption of high efficiency of composite action was developed and utilized to configure two beam specimens, representative of a cross-section of an envisioned longitudinal deck bridge. Construction procedures were conceived and implemented in a time-effective manner. Ramp load test results demonstrated that a high efficiency of composite action resulted – up to 96.4%, thus substantiating the critical design assumption. It was generally evident that the system was considerably stiffer and stronger than expected. Failure was also progressive, leading to a sort of pseudo-ductile (non brittle) overall deflection behavior without collapse. One specimen maintained camber under dead load, one did not. An empirical procedure developed to estimate the time-dependent, creep-like deflection occurring during the 28-day curing period of the concrete proved highly accurate.

Based on the outcomes, further development was recommended, focusing on long-term creep and hygroscopic behavior in time. Rigorous computer modeling to predict such long-term behavior is in progress. Additional beam tests, including cyclic loading over a high number of repetitions, are needed before proceeding to experimental tests on a full-scale longitudinal deck bridge.



# TABLE OF CONTENTS

- 1. INTRODUCTION.....7**
- 2. LITERATURE REVIEW .....2**
  - Theory of Composite Action .....3
  - Efficiency .....5
  - Connections .....5
- 3. BEAM CONSTRUCTION.....9**
  - Instrumentation.....21
- 4. LOAD TESTING .....25**
  - Wood-concrete beam 1 .....26
  - Wood-concrete beam 2 .....34
- 5. DISCUSSION .....40**
  - Time-Dependent Behavior .....41
  - Design Method Verification .....47
  - Efficiency .....53
- 6. SUMMARY AND CONCLUSION.....57**
  - Recommendations .....59
- REFERENCES.....61**
- APPENDIX A .....63**
  - Support Deflection .....63
  - Wood-Concrete Beam 1 .....63
  - Wood-Concrete Beam 2 .....64

## LIST OF FIGURES

Figure 2.1	No Composite Action .....	3
Figure 2.2	Partial Composite Action .....	4
Figure 2.3	Full Composite Action .....	4
Figure 2.4	Efficiency Graph .....	5
Figure 2.5	Description of Hilti Dowel Components .....	6
Figure 2.6	Notched Connection with Hilti Dowel .....	7
Figure 3.1	Elevation View of the Wood-Concrete Beam .....	9
Figure 3.2	Notch at the Support .....	9
Figure 3.3	Utility Pole with a 10-inch Notch Resting on Support .....	10
Figure 3.4	Shim at the Support .....	10
Figure 3.5	Cutting the Shear Key Notch for the Connection .....	11
Figure 3.6	Breaking the Fingers out of the Notch with a Hammer .....	12
Figure 3.7	The Finished Notch after Using the Air Chisel.....	12
Figure 3.8	Cross Section of the Shear Key .....	13
Figure 3.9	Painted Utility Poles .....	14
Figure 3.10	Simpson Model A23 .....	15
Figure 3.11	Lag Bolts at the Corner of the Formwork.....	15
Figure 3.12	Simpson Angle Bracket Model LS30 .....	16
Figure 3.13	Splice along the Formwork.....	16
Figure 3.14	View inside the Form before the Rebar is Installed.....	17
Figure 3.15	Bearing Plate Assembly.....	18
Figure 3.16	Rebar Tie Wire Loop to Hold the Threaded Rod .....	18
Figure 3.17	Rebar Layout.....	19
Figure 3.18	Bottom of the Formwork Showing the Foam Gap Filler .....	20
Figure 3.19	Wood-Concrete Beam and Formwork .....	20
Figure 3.20	Finished Wood-Concrete Beam.....	21
Figure 3.21	Linear Transducers .....	22
Figure 3.22	Slip Measurement Fixture End View.....	23
Figure 3.23	Slip Measurement Fixture Side View .....	23
Figure 4.1	Wood-Concrete Beam Cross Section.....	25
Figure 4.2	Load vs. Deflection of the Wood – Beam 1 .....	27
Figure 4.3	Deflection vs. Time – Beam 1 .....	28

Figure 4.4	Ultimate Strength Test – Beam 1 .....	29
Figure 4.5	Cracking on the Decompression Side of the Inner Notch – Beam 1 .....	30
Figure 4.6	Flexure Crack at Mid Span in the West Utility Pole – Beam 1 .....	31
Figure 4.7	Horizontal Shear Failure in the West Utility Pole – Beam 1 .....	32
Figure 4.8	Load vs. Slip for Ultimate Strength Test– Beam 1 .....	33
Figure 4.9	Partial View of Load vs. Slip for Ultimate Strength Test – Beam 1 .....	33
Figure 4.10	Load vs. Deflection of the Wood – Beam 2.....	34
Figure 4.11	Deflection vs. Time – Beam 2 .....	35
Figure 4.12	Ultimate Strength Test – Beam 2.....	36
Figure 4.13	West Side Cracking at Mid Span around a Knot – Beam 2 .....	37
Figure 4.14	Cracking on the Decompression Side of the Notch – Beam 2.....	38
Figure 4.15	Horizontal Cracks in the East Utility Pole at Mid Span .....	38
Figure 4.16	Tear out of the Tension Face – Beam 2 .....	39
Figure 4.17	Load vs. Slip for Ultimate Strength Test – Beam 2.....	40
Figure 5.1	Mid Span Deflection versus Time for Wood-Concrete Composite Beams 1 and 2.....	42
Figure 5.2	Mid-Span Deflection from Creep versus Time.....	43
Figure 5.3	Deflection from Creep versus Time with a Trend Line.....	44
Figure 5.4	Predicted Deflection for the Wood-Concrete Beams.....	46
Figure 5.5	Percent Error between the Average and Predicted Beam Deflections.....	47
Figure 5.6	Material Property Distribution <sup>26</sup> .....	48
Figure 5.7	Sample Distributions of Load and Resistance <sup>26</sup> .....	49
Figure 5.8	Performance Distribution <sup>26</sup> .....	49
Figure 5.9	Ultimate Loads for Wood-Concrete Composite Beam 1 .....	51
Figure 5.10	Ultimate Loads for Wood-Concrete Composite Beam 2 .....	52
Figure 5.11	Load vs. Deflection plot below the Service Load – Beam 1.....	54
Figure 5.12	Load vs. Deflection plot below the Service Load – Beam 2.....	55

# LIST OF TABLES

Table 4.1	Beam Section Properties .....	25
Table 4.2	Beam Material Properties .....	26
Table 4.3	Concrete Compression Test Data .....	26
Table 5.1	Selected Beam Properties for Creep .....	45
Table 5.2	Summary of Wood-Concrete Composite Beam Loads .....	52
Table 5.3	Summary of Load Margin for the Wood-Concrete Composite Beam .....	53
Table 5.4	Moment and Load Comparison – Wood-Concrete Composite Beam 1 .....	55
Table 5.5	Moment and Load Comparison – Wood-Concrete Composite Beam 2 .....	56



# INTRODUCTION

In 2005, there were 594,187 highway bridges<sup>1</sup> in the United States' official inventory, with 451,843 bridges<sup>2</sup> classified as rural. Additionally, 61,052 of these rural bridges were classified as structurally deficient and another 47,595 bridges were classified as functionally obsolete.<sup>3</sup> Therefore, with 108,647 bridges that need to be replaced or rehabilitated, economical bridge construction techniques are important developments. A potentially cost effective solution for a bridge with a span about 30 feet in length is to use wood-concrete construction.

Wood-concrete construction is not a new idea. For instance, in 1932 the Oregon State Highway Department used this construction system to build a highway bridge.<sup>4</sup> The bridge constructed in Oregon utilized the familiar T-beam shape with creosote treated wood beams providing the tensile strength and a concrete deck providing the compression strength. The bridge was so successful that 198 bridges were constructed in Oregon with wood-concrete composite decks.

While wood-concrete bridge design began in Oregon, it continued in Delaware. Between 1936 and 1938, the Delaware State Highway Department experimented with wood-concrete composite bridges.<sup>5</sup> The bridges in Delaware were designed using a nail-laminated 2" by 8" wood sub deck keyed with a 4" to 8" deep concrete slab. Three bridges were built using the wood-concrete configuration and were designated with the identifiers S-445, S-707, and K-9A. While the K-9A was removed in 1995 due to deterioration, the S-445 and S-707 are still in use after more than 69 years of service. The life span of these bridges is a testament to the durability of wood-concrete structures.

Examining the history of wood-concrete bridge construction one learns that most of its development occurred during the 1930s and 1940s due to the steel shortages of World War II. In 1945, after the war ended, wood-concrete bridge construction was retired in favor of traditional reinforced concrete and steel bridge construction. However, with the turn of the century, labor and material costs increased driving the need for an efficient structure. One of the most structurally efficient designs is one utilizing wood to carry the tensile loads and concrete to carry the compressive loads. Additionally, this system requires minimal formwork and no shoring, allowing a wood-concrete composite bridge to be constructed at a savings of 50 percent over equivalent concrete structures according to the Oregon Highway Department.

In 2000, a move toward green building began, which promoted the construction of more economical and energy efficient structures. This included building structures with materials that had a lower energy usage for production. For instance, a material such as steel has a high-energy usage for production since the iron must be mined, smelted, heated in a blast furnace, cast into slabs, and rolled into the desired shape where each step results in a significant use of resources. Wood, on the other hand, is a natural, renewable resource requiring minimal processing to obtain a usable product. When building a bridge, the cost for demolition and removal at the end of the structure's service life should also be considered. A wood-concrete system is an efficient structure to remove since concrete is kept to a minimum, meaning that less rubble needs to be trucked to the landfill and the wood can be recycled.

The construction process of a wood-concrete system is also advantageous since it requires a minimum of heavy equipment. Average sized utility poles that are 30 feet in length weigh approximately 700 lbs, which are well within the range of a Gradall 544D10-55 variable reach forklift. This allows a bridge over a stream in a deep gully to be constructed without the use of a crane. In addition, since the layered wood-concrete deck bridge proposed herein does not require shoring, it can be constructed without the necessity of applying shores into a moving stream.

Traditionally, large solid sawn pieces of lumber were used on the tension face of the main span and in more recent times, glue laminated lumber has been used. However, finding large pieces of timber to use in a wood-concrete beam can be expensive in today's market. Therefore, an alternative to milled lumber had to be found in order to make wood-concrete as cost effective as possible. One alternative to milled lumber is wood utility poles. Utility poles are effective for use in a wood-concrete bridge system as they are treated with preservatives, made in standard sizes, and are long in length. Additionally, utility companies are routinely removing them for road expansion projects so many are available free of charge.

Wood-concrete construction with the use of utility poles shows great promise. However, research was needed to determine a method of connecting the concrete to the round, tapered utility poles so as to develop effective composite action. Additionally, no design method has yet been developed to predict the service load capacity of such wood-concrete construction. Therefore, it was the goal of this research study to develop a design method to predict the capacity of a representative beam section and then, by performing full-scale load testing, demonstrate that the connections work and a proposed design method adequately predicts the strength of that beam section.

## 2. LITERATURE REVIEW

### 2.1 Theory of Composite Action

Wood-concrete construction first began in the United States when a bridge spanning the canal between the cities of Houghton and Hancock in Michigan was rebuilt in 1929.<sup>6</sup> The bridge was constructed by using 6" x 6" timber cross ties with a precast concrete slab placed on top. This type of construction was chosen because it provided a hardwearing surface and allowed efficient use of the wood. There was no interconnection of the concrete deck to the wood crossties. Thus, this bridge is a "non-composite" system as depicted in Figure 2.1.

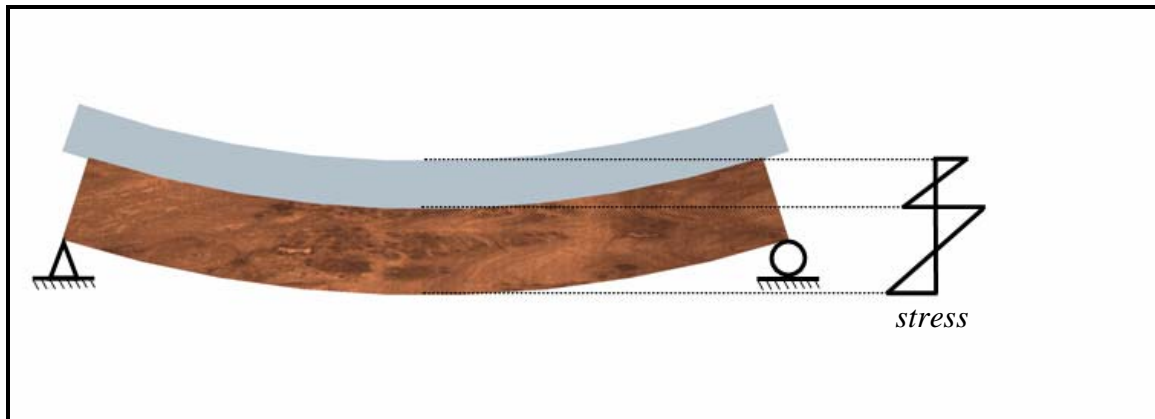


**Figure 2.1** No Composite Action

The mid span stress distribution is shown to the right of the beam and depicts the two independent neutral axes of the wood and concrete layers. The wood-concrete interface, or "slip plane," is the location of the highest tensile stress within the concrete and the largest compressive stress in the wood.

As mentioned earlier, in 1932, the Oregon State Highway Department constructed the first wood-concrete composite bridge.<sup>7</sup> The bridge was constructed by using creosote-treated timber stringers topped with concrete to form a T-beam girder.<sup>8</sup> Interlocking connectors were used between the wood and concrete to provide partial composite action as shown in Figure 2.2. The partially composite system moves the two neutral axes closer together relative to the non-composite case. This transfers more axial tension force to the wood while increasing the axial compression load in the concrete. Additionally, the stresses at the slip plane decrease.

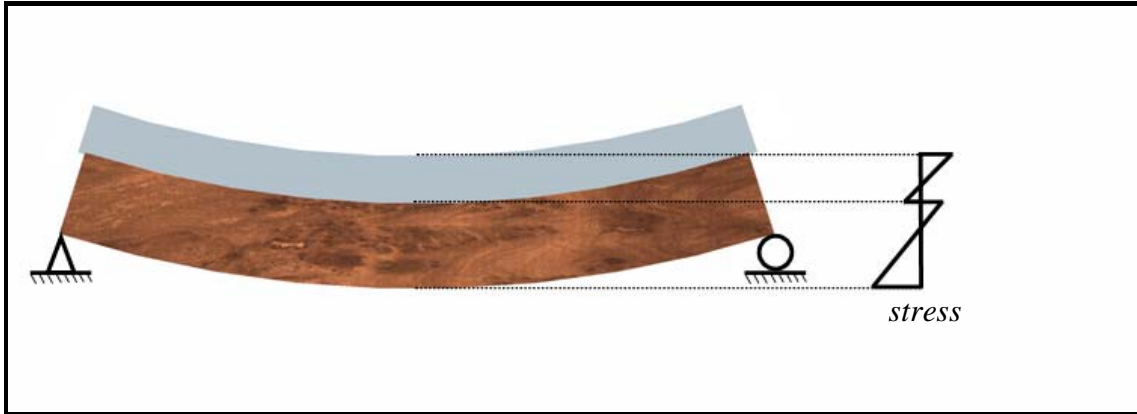


**Figure 2.2** Partial Composite Action

If it were possible to rigidly bond the concrete layer to the wood layer, full composite action would result. A way to achieve this type of bond would be to cast and cure the slab separately, applying a “rigid adhesive” to the wood beam and then use a crane to place the slab on the wooden beams. However, due to the natural variability in the wood and the way the concrete is cast, there is no guarantee that the wood beam and the concrete slab will lie flat against the wood. Additionally, to move the slab would require flexural reinforcement to be purchased and installed to keep the slab from cracking under its own weight, and that could be cost prohibitive. Despite the problems with gluing the wood and concrete layers together, Pincus<sup>9</sup> was able to create a partially composite bond between the wood and concrete through the use of an epoxy. However, he encountered similar problems as described above with the bonding of the layers, moisture, and inability of the bond to withstand impact tests. At the University of Singapore, an epoxy resin was used to connect a concrete slab to wooden stems.<sup>10</sup> The wood-concrete composite beam exhibited nearly full composite action during ramp loading, however, the cost of the epoxy resin was so high that it made this connection method impractical. The idealized and highly sought after full composite action is shown in Figure 2.3.

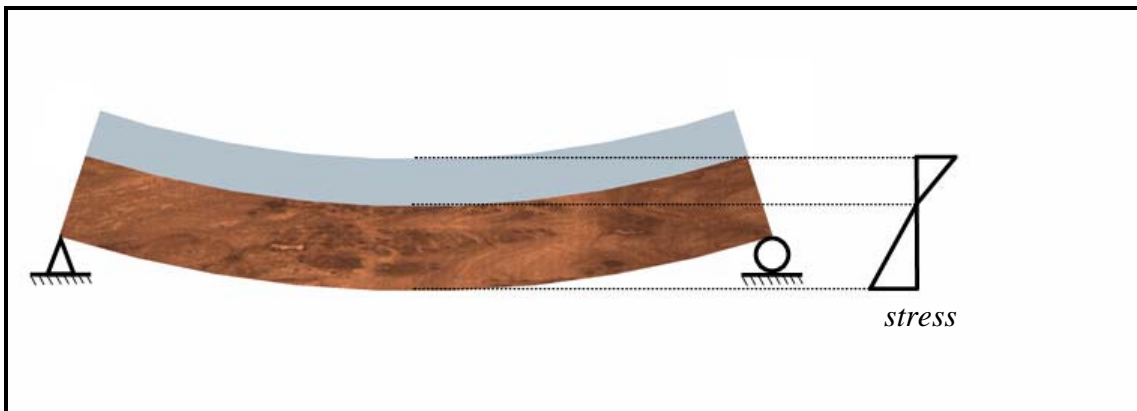


**Figure 2.3** Full Composite Action

For full composite action there is only one neutral axis for the beam, and this axis is typically placed along the slip plane between the wood and concrete layer. The beam can be analyzed by using the method of transformed sections to determine the neutral axis and the stresses in the beam.

## 2.2 Efficiency

The amount of the horizontal shear force transferred between the wood and concrete slip plane determines the efficiency of the composite system. Herein, efficiency will be determined using a relationship given by Pault:<sup>11</sup>

$$EFF = \frac{\Delta_N - \Delta_P}{\Delta_N - \Delta_C} \quad \text{Eq 0.1}$$

Where  $\Delta_N$  is the theoretical non-composite deflection,  $\Delta_P$  is the measured composite deflection, and  $\Delta_C$  is the theoretical composite deflection. Efficiency quantifies the degree of composite action, where 100% efficiency is full composite action. The efficiency of a beam is inversely related to interlayer slip, which is the relative movement of the wood and concrete layers at the interface. As slip increases the composite efficiency decreases. However, the relation of slip to composite action changes with the beam configuration and span. Therefore, it is more convenient to use efficiency as a way to describe how close a beam is to achieving fully composite action over the slip measurement. Figure 2.4 illustrates the relationship between full, partial, and non-composite action.

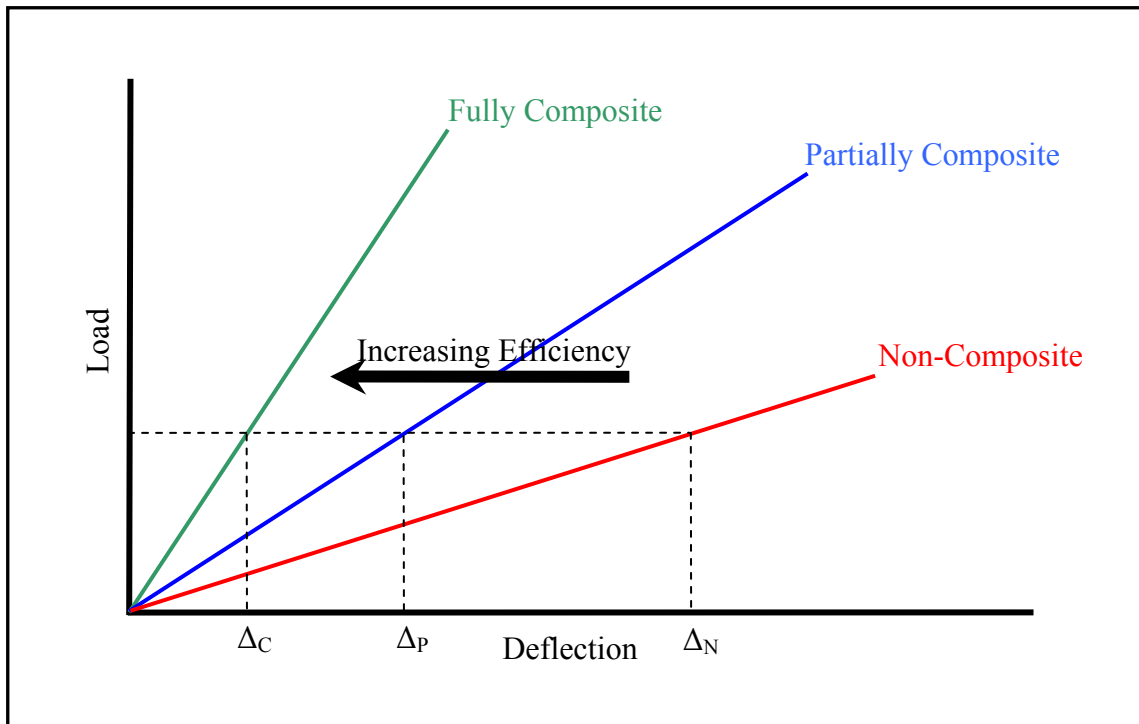
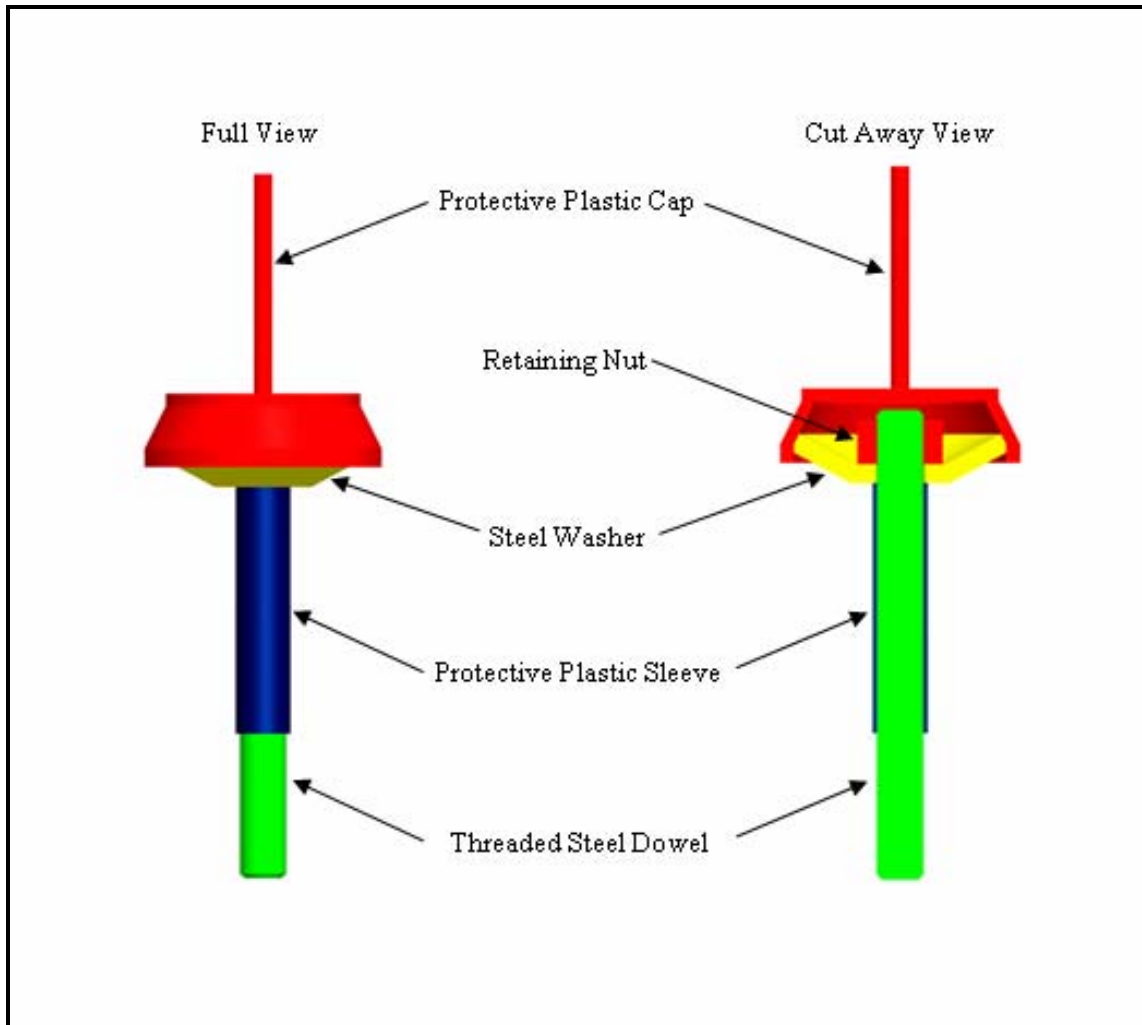


Figure 2.4 Efficiency Graph

## 2.3 Connections

A type of connection originally developed by Natterer et al.,<sup>12</sup> which uses a shear key and Hilti dowel anchor, was adapted to this research. The main advantage of this system is that the anchor can be post tensioned after the concrete has been cast and cured. The post tensioning forces the concrete up against the wood ensuring a positive connection and increasing friction between the wood and concrete layer. In a typical installation, there are five pieces to the dowel assembly as shown in Figure 2.5.



**Figure 2.5** Description of Hilti Dowel Components

The first piece is the protective plastic cap that protects the retaining nut and upper dowel threads from being covered by concrete when the concrete slab is poured over the wood beam (see Figure 2.6). The plastic cap also has a breakaway tab on top attached to the marker so there is easy access to the retaining nut for post tensioning. The washer has an angular shape to help avoid air pockets while the concrete is filling around the dowel.

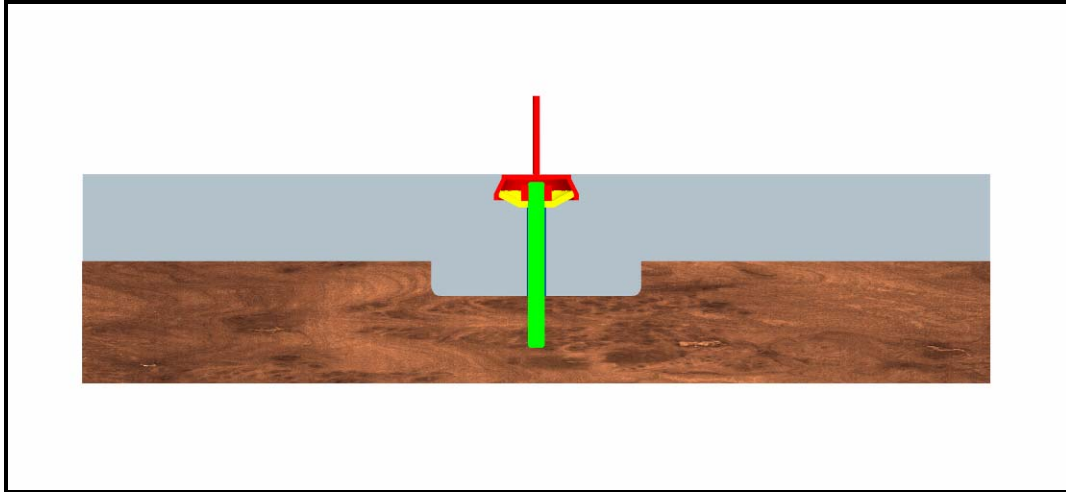


**Figure 2.6** Notched Connection with Hilti Dowel

The dowel is made of steel all-thread and is long enough to penetrate the wood three inches while the top of the protective cap is flush with the surface. To maintain the integrity of the threads and allow the concrete to move relative to the dowel, a plastic sleeve of 0.5" ID clear vinyl tubing is placed over the dowel where it is exposed to the concrete between the wood and bottom of the steel washer. To anchor the dowel to the wood, a two-part epoxy is used to bond the metal dowel to the wood. Four different types of epoxies have been used to bond the dowel to the wood, including the Hilti C-50 HIT WTR adhesive, Hilti HIT HY 150 adhesive, and a laminated resin produced by Borden Chemical Inc. The results of tests conducted using this adhesive are shown in the thesis by Brown.<sup>13</sup> The most recent type of epoxy used to secure the Hilti dowels to the wood beam was an epoxy made by West Systems. The epoxy required the 104-resin to be mixed with the 206-hardener in a 4:1 ratio. Wood-concrete composite beam tests on 12-foot long wood-concrete floor beams showed that the resin provided adequate strength to bond the Hilti dowel to the wood. The main purpose of securing the dowel with an epoxy is to prevent any metal connectors from exposure on the underside of the beam. This increases the fire protection of the connection for use in a residential floor system. If the connector is used for an exterior bridge, the dowel could be run to the underside of the beam and secured with a bearing plate, washer, and nut.

The shear notch for the connection, as shown in Figure 2.6, can have either vertical sides or angled sides. However, this does not affect the efficiency of the connection. With this type of connection, efficiencies of 83.4% - 96.4%, based on the testing performed herein and from load testing performed on 12-foot wood concrete beams composed of laminated 2x4s can be achieved depending on the concrete mix design.<sup>14</sup> The concrete composition is important since a high strength and high slump concrete mix is required to fill the shear key properly. It is important to note that the stiffness of this connection is mainly due to the shear key created between the wood and the concrete. The transfer of the horizontal shear forces through the concrete and directly into the wood instead of with an intermediate mechanical connection increases the rigidity of the connection.

The dowel used in this connection is not intended to take significant horizontal shear force and should primarily receive the upward tensile force caused by the slab wanting to lift off the concrete due to flexure as well as the upward component of force caused by the angle of the notch. In past studies, researchers have noticed gaps in the shear key between the wood and concrete bearing surfaces as indicated by Brown. This caused the concrete to slip up against the wood as the initial live load was placed on the wood-concrete beam and caused the Hilti dowel to receive a horizontal component of force, i.e., to be stressed in shear.



### 3. BEAM CONSTRUCTION

To overcome the dead load deflection of the beam due to the weight of the concrete and utility poles, it is critical to have camber in the beam. The camber on the underside of the wood-concrete composite beam is natural and comes from the tapered shape of the utility poles and their placement as shown in Figure 3.1.

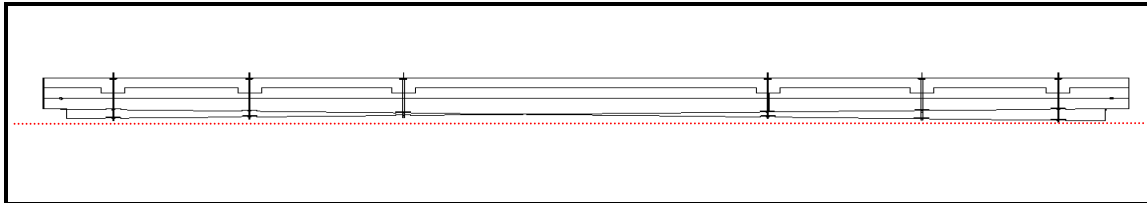


**Figure 3.1** Elevation View of the Wood-Concrete Beam

To create camber, the tops of the logs are placed level relative to each other so that a natural arching occurs on the underside of the utility poles. However, since the utility poles are different diameters at the ends, a notch in the larger end of the utility poles is created as shown in Figure 3.2. The support notch depth is determined by measuring the difference between the end diameters and cutting the notch to that depth. Measure down from the top of the utility pole and place a mark at a distance equal to the difference in diameters on the end of the utility pole. Using a level, a horizontal line is drawn at the end of the beam. The width of the supports on the load frame is 8 inches, so with a 2-inch overhang at the end of the support a 10-inch long notch is cut. After the notch is cut, the utility pole is rolled over so that the 10-inch notch rests on the support as shown in Figure 3.2 and Figure 3.3.



**Figure 3.2** Notch at the Support



**Figure 3.3** Utility Pole with a 10-inch Notch Resting on Support

Notching the utility poles at the end creates a uniform look, but it may not be the best choice if there are high vertical shear loads at the support. If high shear loads exist at the notch, a better solution is to shim the smaller log so that its top is level with the larger utility pole as shown in Figure 3.4.



**Figure 3.4** Shim at the Support

After both utility poles are notched and placed to create the camber, the ends are horizontally pinned together with a three-quarter inch diameter piece of steel all thread (see Fig. 3.3). After placing the concrete, this pin is not structural, however, it does keep the ends of the logs together while cutting the connection notches and installing the formwork.

Figure 3.1 illustrates how the end notching process achieves camber in the lower portion of the beam. However, the concrete deck remains flat without any camber. This is done purposely to make formwork easier to install and to provide a uniform compression area throughout the length of the beam. If the deck is installed in the field, it should be asphalted to create a flat surface and fill in any sag in the center of the

span due to the beam's dead load. The asphalt deck will provide the concrete protection from road hazards since a chunk of concrete removed from the deck at the centerline of the span could make the beam structurally inadequate. The asphalt deck provides an extra margin of safety.

Next, the twelve shear key notches in the two utility poles are cut. The notch locations are marked at the crest of the utility pole by measuring from the end of the beam. Then a circular saw is set at the notch angle and depth of the notch. Two opposing cuts are made to create the outer dimensions of the notch for the shear key. Then a series of cuts are made between the two outer cuts as shown in Figure 3.5.



**Figure 3.5** Cutting the Shear Key Notch for the Connection

It is important to keep the saw level on the round utility pole so that a uniform depth is created along the width of the notch. The wood fingers left from the series of cuts are then being knocked out with a hammer to form the notch as shown in Figure 3.6. Using an air chisel, any remaining material should be removed from the notch (see Figure 3.7).

Next, a hole is drilled 1/16 of an inch greater than the nominal size of the threaded rod in the center of each notch so the Hilti dowel can pass through the center of the utility pole. Using this hole as a guide, a notch for the bearing plate is cut on the underside of the pole to provide a flat bearing surface using the same notching technique described earlier for the shear key notch. A cutaway schematic of the shear key, Hilti dowel, and bearing plate is shown in Figure 3.8.



**Figure 3.6** Breaking the Fingers Out of the Notch with a Hammer



**Figure 3.7** The Finished Notch After Using the Air Chisel

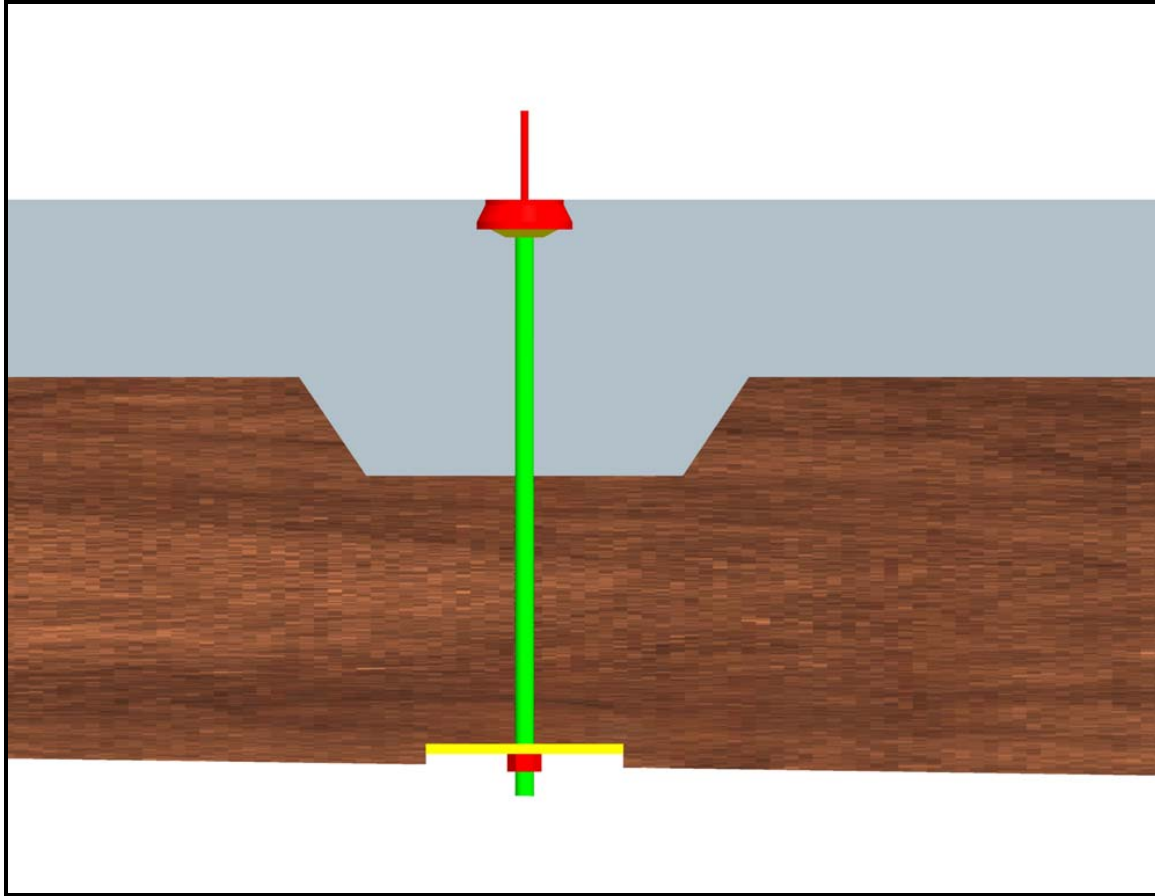


**Figure 3.8** Cross Section of the Shear Key

The adjacent utility poles will have gaps in places along the length of the beam. If the gap is greater than one-half inch wide, it is filled by cutting a tapered wedge with the table saw and sliding it between the logs. The wedge is then secured with Bondo®. For gaps between the logs smaller than half of an inch, the gaps are filled with Bondo® alone. It is important that no gap is larger than one-fourth of an inch between the logs since the concrete that will be placed on top of the logs has a high slump and will run out of a larger gap.

If concrete was placed directly on the bare wood of the utility poles, the wood fibers would wick away moisture from the concrete causing the concrete to dry cure and the wood to swell. The swelling of the wood from water absorption works against the efficiency of the connection. The main problem occurs when the wood swells and compresses the uncured concrete. When the wood dries and reaches stable moisture content, there is a gap between the wood and the concrete, which adds an initial slip to the beam and a reduced stiffness. To keep the swelling of the wood from occurring, a waterproof paint is applied to the utility poles. UGL Drylock oil based waterproofer has been found to be effective for this situation. Traditionally, Drylock is used to prevent water seepage through basement walls, and it works equally well at preventing water from penetrating the wood. The paint is applied using a roller and brush. However, if a number of poles needed to be painted, an airless sprayer can be used to apply the paint more efficiently. Around the circumference of the utility poles, natural checking from the wood drying over the years caused deep gaps in the wood. If left unsealed, they would allow moisture to enter the utility poles. Therefore, on the top side of the utility poles where the concrete would be in direct contact with the wood, paint was forced into the cracks with a brush to ensure adequate coverage. The painted utility poles are

shown in Figure 3.9. The entire utility pole was painted in an attempt to stabilize the moisture content of the utility poles. This may or may not have been necessary.



**Figure 3.9** Painted Utility Poles

The UGL Drylock oil based waterproofer goes on thick and requires a drying time of 24 hours before the formwork is installed. The formwork was designed not to require shoring. Most traditionally built reinforced concrete beams require shoring to support the beam's dead weight as the concrete cures. However, when a bridge needs to be constructed over a river or deep gully, shoring can be very difficult or impossible. Yet, with a wood-concrete beam, the formwork can be attached directly to the utility poles. Then, when the concrete is placed, the utility poles support the dead load of concrete. The absence of the need for external shoring is an important factor in the economics of this concept.

Brackets commercially available from Simpson Strong Tie were used to connect the formwork to the utility poles. Two of the Simpson model number A23 angle connectors were used at each end of the utility poles to hold up the ends of the formwork as shown in Figure 3.10. The forms were constructed of nominal 4" x 12" boards (3½" x 11¼" actual) since this allowed for an 8-inch slab with an 1¼-inch cover over the side of the utility pole. Three-inch long number eight drywall screws with a fine thread were used to attach the Simpson bracket to the utility pole, and 2-inch long number six drywall screws with a fine thread were used to attach the Simpson bracket to the form.



**Figure 3.10** Simpson Model A23

The corners of the forms were joined horizontally using 3/8" by 8-inch lag bolts. The corner connection of the formwork is shown in Figure 3.11. To keep the lag bolt from binding in the wood, a 3/8" clearance hole was first drilled through the longitudinal form and then a 3/16" pilot hole was drilled in the transverse end form. Two lag bolts were used at each corner spaced three inches from the top and bottom of the form. Angled support brackets were used to support the formwork along the length of the utility pole (see Figure 3.12). They are also manufactured by Simpson Strong Tie and have a model number of LS30. These brackets can be bent to conform to the round shape of the utility pole.



**Figure 3.11** Lag Bolts at the Corner of the Formwork



**Figure 3.12** Simpson Angle Bracket Model LS30

The wood boards used for the formwork are only 12 feet long so it was necessary to make splices along the length of the wood-concrete beam. The splices are created by nailing nominal 2X6 boards to the side of the beam. Then a flume brace is used to support the sides of the formwork (see Figure 3.13). Figure 3.14 shows a view inside the form before installing the rebar.



**Figure 3.13** Splice Along the Formwork



**Figure 3.14** View Inside the Form Before the Rebar is Installed

Now the Hilti dowels are installed using the assembly procedure shown in Figure 2.5 with the exception of the plastic sleeve. Due to the high horizontal shear load at the shear key, the steel must be in contact with the concrete to provide adequate clamping force between the shear planes. However, because of this modification, the Hilti dowel needs to be tightened to 25 foot-pounds of torque from the top and bottom to pull the concrete securely against the wood.

The threaded rod used for the Hilti dowel is cut using an abrasive cutoff wheel, horizontal band saw, or hacksaw. The researchers found it easiest to cut all of the dowels at the same time to the longest required length and then trim any excess below the bearing plate after the concrete has cured. To keep the Hilti dowel's washer tight against the nut, a loop of rebar tie wire is tied to the dowel under the washer. This step keeps the washer and protective cap in the proper position while the concrete is placed in the form. The flat top of the red protective plastic cap should be flush with the top of the forms so that once the concrete has cured, the top of the cap can be removed and the nut torqued to 25 foot-pounds. The access hole is then grouted before the asphalt topping is applied. Once the washer, nut, and protective cap are secured to the threaded rod with rebar tie wire, the assembly is placed in the notch hole drilled earlier and the bearing plate, nut, and washer are secured as shown in Figure 3.15. To keep this entire Hilti dowel assembly from sliding through the hole, another loop of rebar tie wire is placed where the threaded rod enters the notch hole (see Fig. 3.16).



**Figure 3.15** Bearing Plate Assembly



**Figure 3.16** Rebar Tie Wire Loop to Hold the Threaded Rod

In the beam shown in Figure 3.17 there are three longitudinal pieces of rebar shown as they are required to meet the minimum reinforcement requirements. Two pieces of rebar are tied to the Hilti dowels to provide 1.5 inches of cover for the transverse reinforcement that was tied on top of the longitudinal reinforcement. Then the third longitudinal bar is attached below the transverse reinforcement. The third longitudinal bar was placed in the center between the other two longitudinal pieces of rebar to ensure even distribution of the reinforcement. Then the transverse reinforcement is placed. The transverse reinforcement was spaced to meet the ACI design requirements for minimum reinforcement, which requires a #3 bar placed every 7.5 inches on center.



**Figure 3.17** Rebar Layout

With all of the reinforcement installed, any gaps between the formwork and the utility poles were filled with Great Stuff®, which is an expanding foam sealer used to fill gaps in houses. The foam is waterproof and bonds to anything, which makes it a great product for filling gaps in the forms. Bondo® should not be used to fill the gaps between the utility poles and the formwork since it creates a permanent bond, making the formwork more difficult to remove after the concrete has been placed. Figure 3.8 shows the sealed forms.

The forms were then covered with a release agent. Any commercial release agent will work, but simply spreading used motor oil on the forms worked well. The motor oil fills the pores of the wood to keep the wood from absorbing water from the concrete. Additionally, the oil prevents the concrete from sticking to the formwork, making form removal easy. Figure 3.19 shows the complete beam and formwork ready for concrete placement.



**Figure 3.18** Bottom of the Formwork Showing the Foam Gap Filler



**Figure 3.19** Wood-Concrete Beam and Formwork

The concrete is placed into the forms with the aid of a Bobcat skid steer loader. After the concrete is cured for one day, the forms are removed to reveal the finished wood-concrete composite utility pole beam shown in Figure 3.20.



**Figure 3.20** Finished Wood-Concrete Beam

### **3.1 Instrumentation**

Two linear displacement transducers were placed at each of three points along the beam so that the deflection of each utility pole could be measured independently. One set of transducers was placed at each support of the beam and one set was placed at the mid span of the beam. The mid span transducers are shown in Figure 3.21. To prevent the transducers from moving during the experiment, they were anchored to the concrete using plastic anchors and screws.

It is important to measure the slip between the wood and concrete layer to determine the effectiveness of the shear key. The location of the most slip between the wood and concrete layer is at the end of the beam. Therefore, the researchers configured a fixture able to read the average slip of the two utility poles relative to the concrete. The fixture contains two pieces – the first piece is made of 3/8" plate and attaches directly to the concrete slab using plastic anchors and screws (see Figure 3.22).



**Figure 3.21** Linear Transducers

The second piece of the fixture is a piece of two by four by quarter inch wall tubing that is welded to two one inch stand offs and is screwed to the back of the utility poles using three inch number eight drywall screws. Then a magnetic base is mounted to the steel plate attached to the concrete. This magnetic base was special-made to hold a dial indicator rigidly in any position. The Mitutoyo dial indicator used to take the relative measurements between the wood and concrete has an accuracy of 0.0001 inches and a range of one-half inch. With the indicator mounted to the magnetic base as shown in Figure 3.23, the indicator will read backwards since the concrete is moving away from the wood.

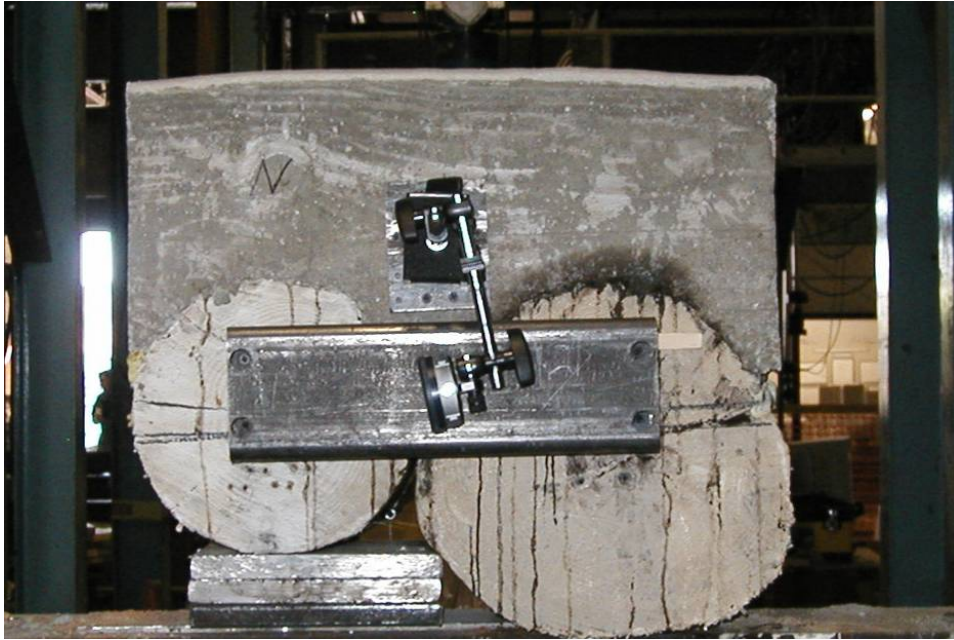


**Figure 3.22** Slip Measurement Fixture End View



**Figure 3.23** Slip Measurement Fixture Side View



## 4. LOAD TESTING

Two wood-concrete composite beams were constructed of utility poles and load tested to failure by placing the beam in three-point bending. The general cross section of the beams is shown in Figure 4.1 and the dimensions of Wood-Concrete Beam 1 and Wood Concrete Beam 2 are listed in Table 4.1. This cross-section represents a typical cut from a much wider complete longitudinal deck bridge.

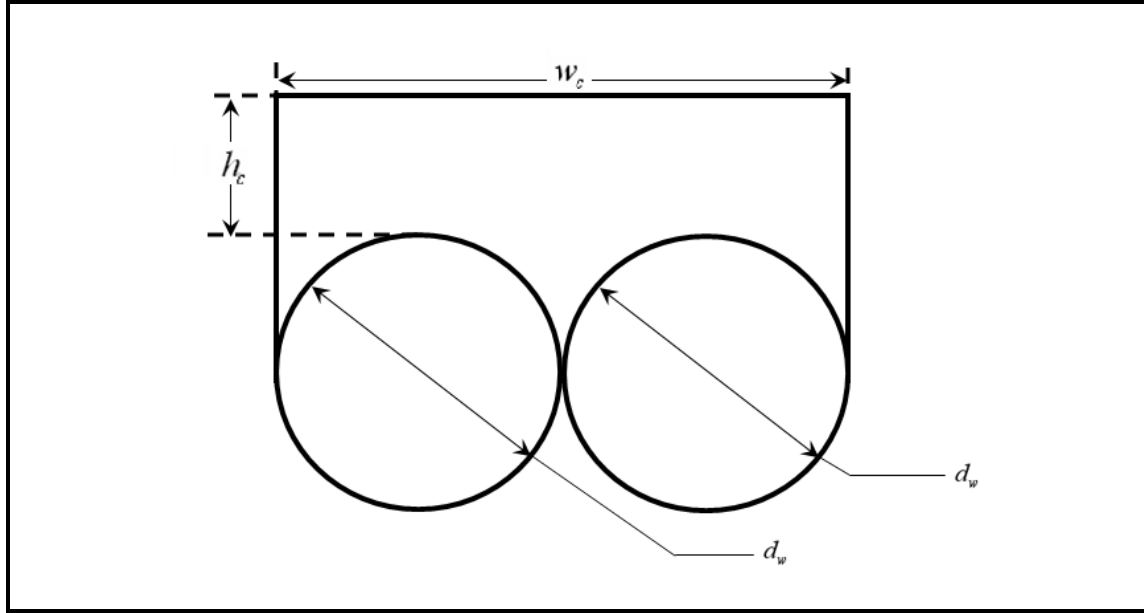


**Figure 4.1** Wood-Concrete Beam Cross Section

**Table 4.1** Beam Section Properties

	Wood-Concrete Beam 1	Wood-Concrete Beam 2
Diameter of the Wood	$d_w = 11.875 \text{ in}$	$d_w = 10.0 \text{ in}$
Height of the Concrete	$h_c = 6.0 \text{ in}$	$h_c = 8.0 \text{ in}$
Width of the Concrete	$w_c = 23.75 \text{ in}$	$w_c = 20.0 \text{ in}$
Span Length	$L = 354.24 \text{ in}$	$L = 354.24 \text{ in}$

Many of the design features of the two wood-concrete beams were the same, yet they had some differences. The section properties of the two beams are shown in Table 4.2. The utility pole in the first beam constructed had an average diameter 18.75% larger than the second beam. The modulus of elasticity determined from tests described subsequently were also different for each utility pole. The average modulus of elasticity of the two utility plies in the first beam was 56.3% of those of the second beam. The beams also had different moments of inertia for the transformed section. The different moments of inertia were a result of the different average diameters and having different modular ratios. The concrete height of the first beam was reduced to the limit of keeping the neutral axis from being located below the crest of the wood, and the concrete height of the second beam was increased to the limit of preventing the initial dead load deflection from exceeding the amount of available camber in the beam. Even though adjustments were made to the concrete length to prevent a large variance between the moments of inertia, the resulting moment of inertia of the first beam's transformed section was still 41% larger than that of the second beam.

**Table 4.2** Beam Material Properties

	Wood-Concrete Beam 1	Wood-Concrete Beam 2
Density of Concrete	$\rho_{c1} = 0.150 \text{ kips/ft}^3$	$\rho_{c2} = 0.150 \text{ kips/ft}^3$
Area of the Concrete	$A_{c1} = 172.76 \text{ in}^2$	$A_{c2} = 181.46 \text{ in}^2$
Fully Composite Moment of Inertia	$\bar{I}_1 = 16084.38 \text{ in}^4$	$\bar{I}_2 = 11348.65 \text{ in}^4$
Modulus of Elasticity for the Wood	$E_{w1} = 1.1065 \cdot 10^6 \text{ psi}$	$E_{w2} = 1.966 \cdot 10^6 \text{ psi}$
Moment of Inertia of the Wood Utility Poles	$\bar{I}_{w1} = 1952.25 \text{ in}^4$	$\bar{I}_{w2} = 981.75 \text{ in}^4$

Standard cylinders were cast for each beam at the time the concrete was placed in the forms in order to later determine the 28-day compression strength of the concrete. The concrete cylinders were loaded at 30 psi/second. The breaking stress of each cylinder is shown below in Table 4.3. The average compressive strength of the three concrete cylinders for Wood-Concrete Beam 1 is 5311 psi and the average compressive strength of the concrete used in Wood-Concrete Beam 2 is 5075 psi.

**Table 4.3** Concrete Compression Test Data

Cylinder	Wood-Concrete Beam 1	Wood-Concrete Beam 2
	Maximum Compressive Stress $f'_c$ (psi)	Maximum Compressive Stress $f'_c$ (psi)
1	5217	5075
2	5700	5040
3	5016	5111

## 4.1 Wood-Concrete Beam 1

Before adding the concrete layer, the utility poles were tested alone to determine their modulus of elasticity values. After the support notches were cut and the ends of the utility poles pinned with a threaded rod, a single hydraulic actuator load was applied at mid span and transferred equally to each utility pole with a spreader beam. Linear displacement transducers monitored the deflection of the beam. During the three-point bending tests to failure, the deflection adjacent to each support was monitored so that mid span deflection could be adjusted to reflect any vertical displacement of the beam at the supports. The support correction was completed by measuring the mid span deflection at each utility pole and then subtracting the average of the specimen's end support deflections. Knowing the load, deflection, and moment of inertia of each utility pole allowed for the modulus of elasticity for each utility pole to be empirically calculated from the applicable mechanics equation for deflection under the mid span loading

used, namely  $\Delta = \frac{PL^3}{48EI}$ . The slope of the plotted  $P - \Delta$  results was used for  $P/\Delta$ . The average of the

two values for the utility poles was taken as the modulus of elasticity for the specimen. In these tests there were no shear key notches cut into the utility poles. Figure 4.2 shows the plots of measured load versus mid span deflection corrected for any support displacement the two utility poles.

The utility poles used in this project were donated from a local utility company when a road was widened in the area. Therefore, the researchers did not have a choice of their species or size. The east utility pole

is Ponderosa Pine and the west utility pole is Western Red Cedar. It is evident from the load versus deflection curve in Figure 4.2 that there is a variance in the stiffness of the two utility poles. The modulus of elasticity values determined from the load tests were 1,255 ksi and 958 ksi for the east and west utility poles.

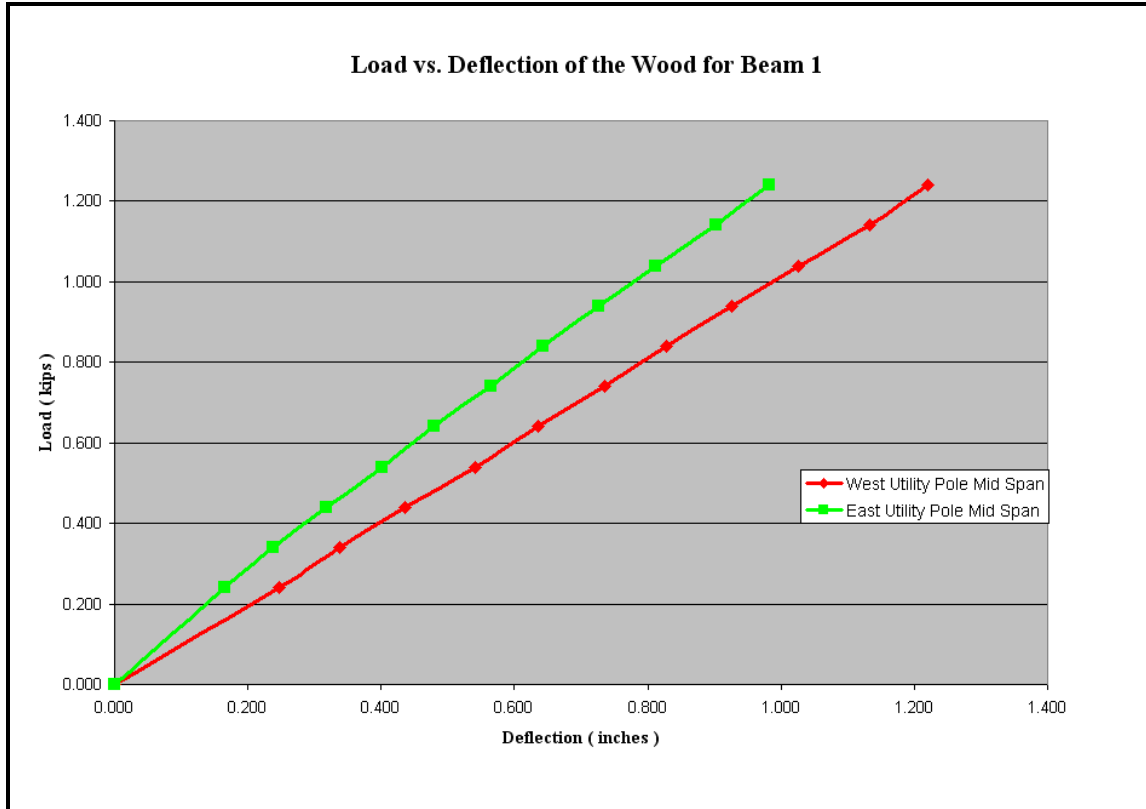


**Figure 4.2** Load vs. Deflection of the Wood – Beam 1

After determining the modulus of elasticity of each utility pole, the concrete layer was placed. The support and mid-span deflections of the beam under its own dead weight were monitored over a 28-day period as the concrete cured. The relative humidity was also monitored using data from the Chrisman Field Weather Station, which is located a quarter mile from the laboratory where the load tests were performed. Figure 4.3 shows the resulting mid span deflection (adjusted for support effects) for the entire 28 day period of curing and the trend in relative humidity. In Fig. 4.3, the datum point at time zero is the point before any concrete was added to the beam. The next datum point at 0.2 days is the initial deflection more or less immediately after the concrete was added. The points up to the 28<sup>th</sup> day show the movement of the beam due to the time-dependent effects of shrinkage of the concrete, creep of the concrete, creep of the wood, and fluctuations in relative humidity. It is evident that at the time the concrete was placed in the formwork the west utility pole deflected more than the east utility pole. This is due to the lower modulus of elasticity of the west utility pole. Once the curing process began to harden the concrete, the two utility poles were bonded to the concrete slab and deflected in unison.

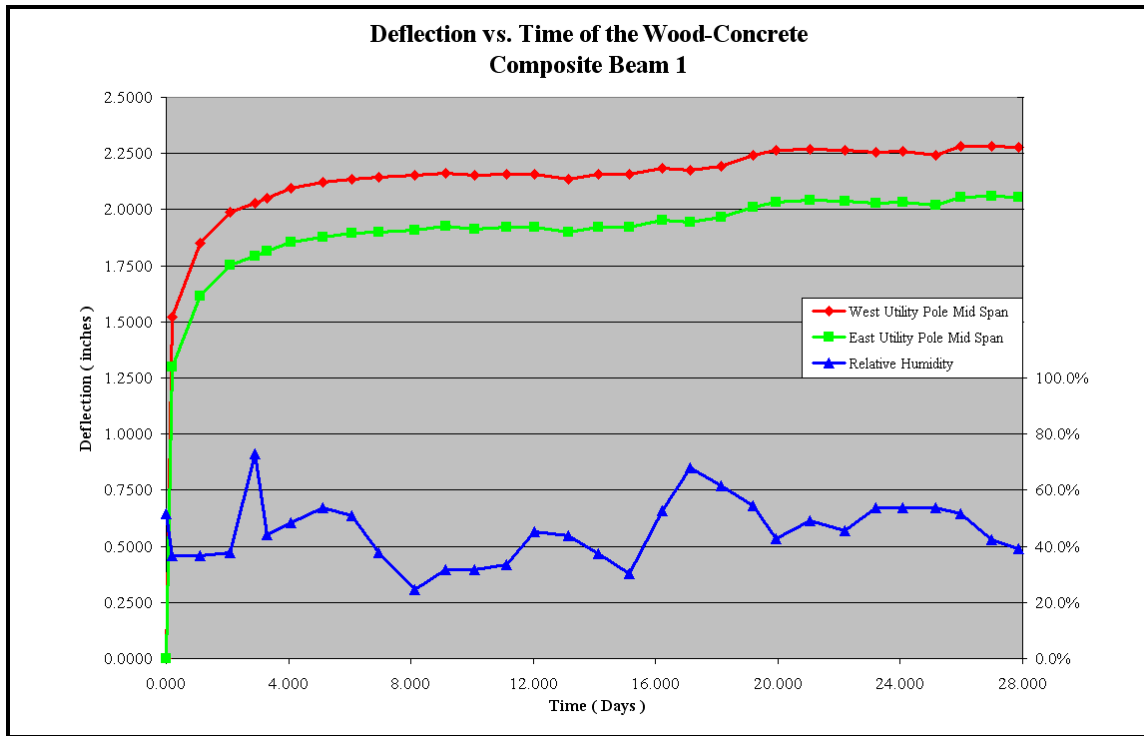


**Figure 4.3** Deflection vs. Time – Beam 1

Immediately after the 28-day curing period, the wood-concrete beam was ramp loaded at mid span to observe the beam’s ultimate load capacity in a point load configuration. The load was applied at mid span using a spreader beam to distribute the load over the wood-concrete beam’s width. A pivot point was centered above the spreader beam so that if the utility poles deflected by different amounts, a uniform load distribution across the width of the beam could still be maintained. Figure 4.4 shows the results of the load test after adjusting for support effects. Graphs of load-deflection responses of the two wood-concrete beam specimens without adjustments for end support deflections are included in Appendix A. Hereafter, all graphs shown will have that adjustment already included.

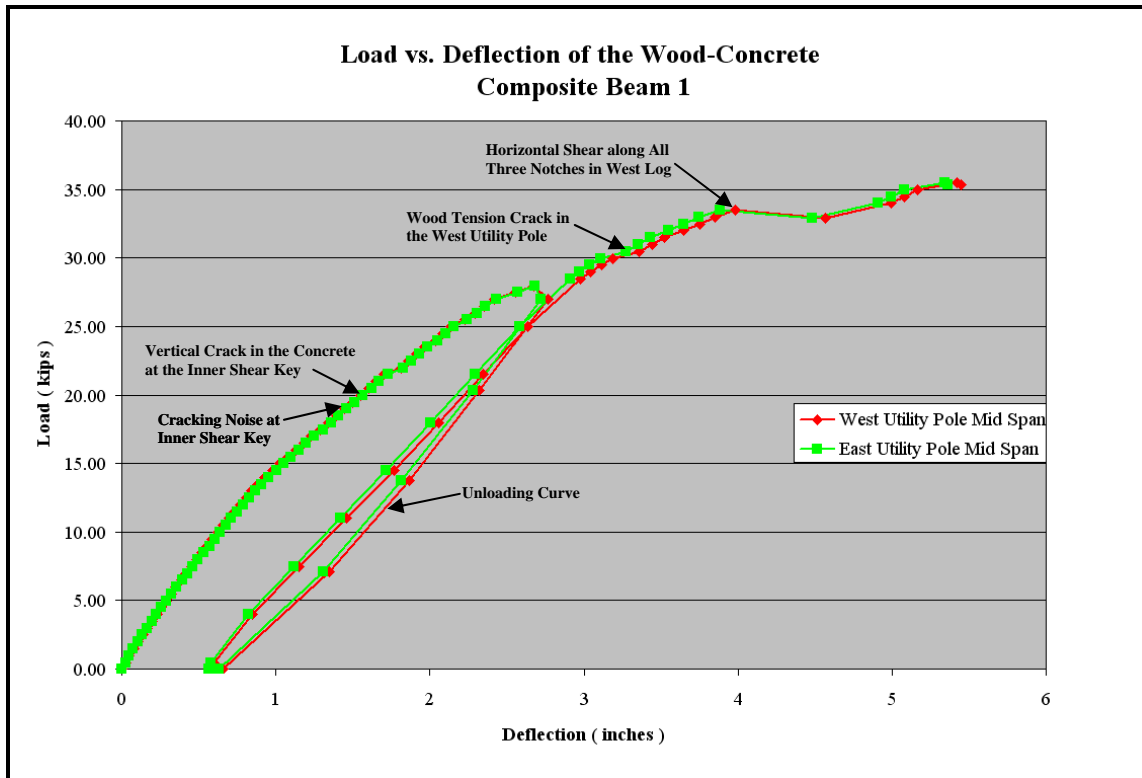


**Figure 4.4** Ultimate Strength Test – Beam 1

It is evident that once the concrete had cured, the two utility poles deflected together under load. The sequence of events that lead to the first noticeable failure of the beam began with flexural cracking at the inner most shear key. At 19.48 kips, there was an audible cracking noise coming from the wood at the inner shear key as shown in Figure 4.4. Then, at 20.55 kips, the concrete at the inner notch began cracking on the unloaded side of the shear key. This created the hooked flexural crack drawn in black and shown in Figure 4.5. For purposes of identification, the notch position and direction of forces acting on the shear key notch and Hilti dowel are drawn over the concrete.



**Figure 4.5** Cracking on the Decompression Side of the Inner Notch – Beam 1

At 27.98 kips, the load was removed from the beam so that an unloading curve could be plotted, providing a graphical representation of how much stiffness the beam would have after being loaded to 1.7 times its factored design load capacity.<sup>19</sup> It can be seen that the beam had a residual deflection of 0.566 inches at mid span after having deflected 2.68 inches at the 27.98 kips load level. The ramp loading back up to 27.55 kips was uneventful. However, at 30.48 kips, a flexural crack in the lower tensile fiber of the beam formed around a knot 12 inches from the mid span of the beam (see Figure 4.6). Vertical flexural cracks also appeared at the mid span of the beam below the neutral axis of the concrete.

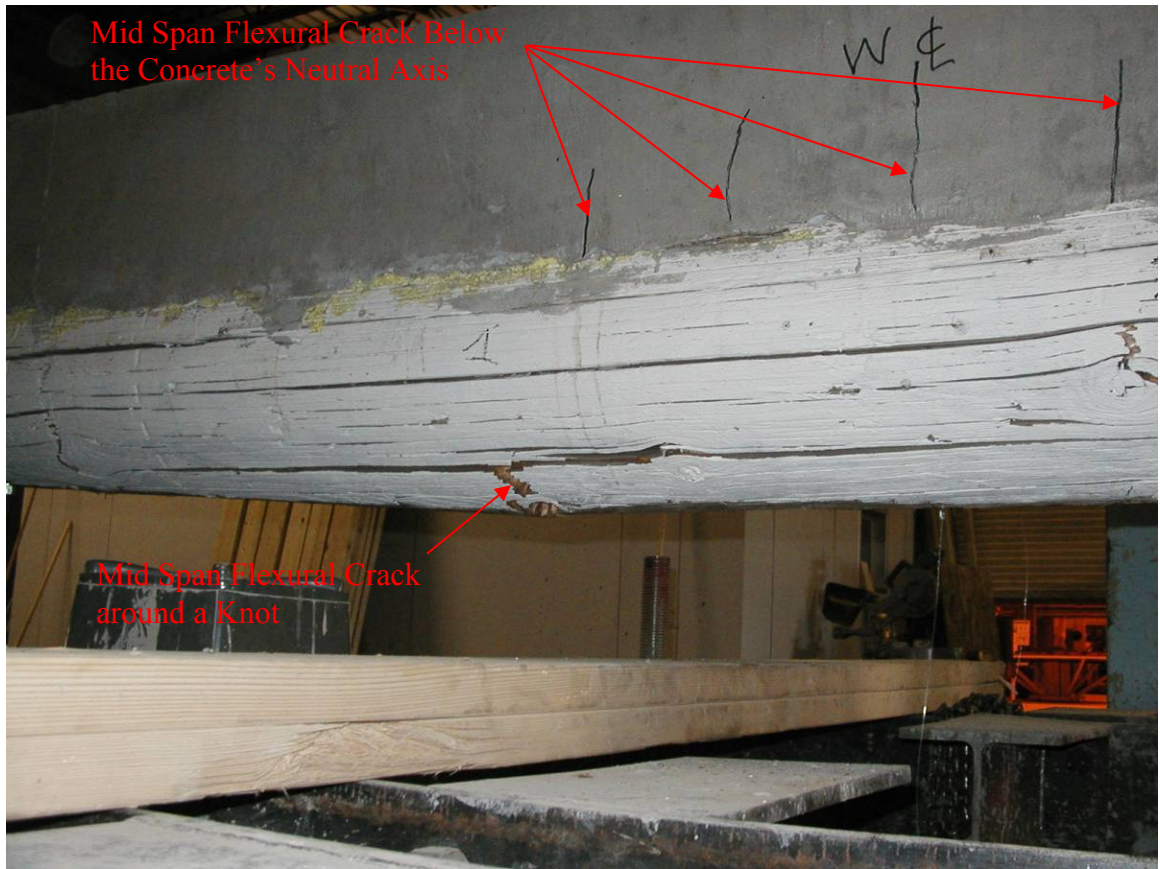


**Figure 4.6** Flexure Crack at Mid Span in the West Utility Pole – Beam 1

At 33.48 kips, the west utility pole experienced a block shear failure at the south end as shown in Fig. 4.7. As only the end of the utility pole was visible, it is not known if this crack extended only to the first notch or affected the other notches. When the shear failure occurred, the beam lost stiffness, causing the beam to deflect 1.48 inches with only a 2-kip increase in load. Once the beam reached a maximum deflection of 5.45 inches, the actuator travel was fully exhausted and the loading ceased.

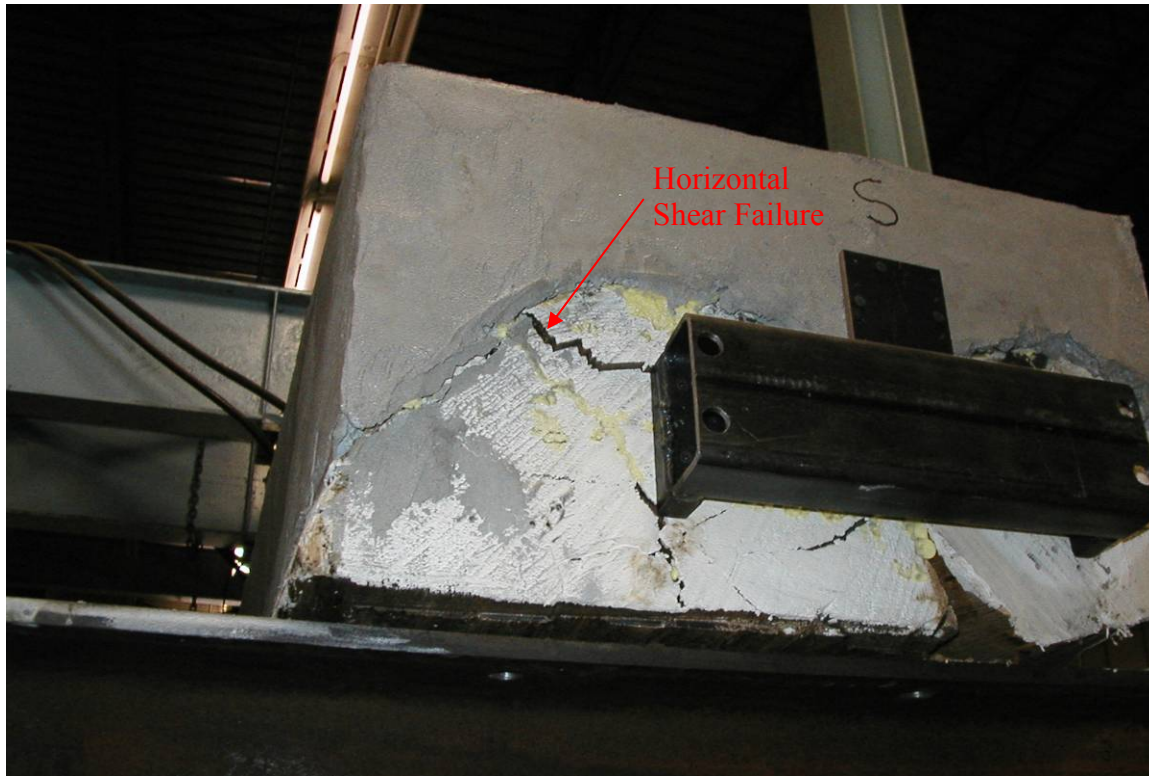


**Figure 4.7** Horizontal Shear Failure in the West Utility Pole – Beam 1

Slip at each end of the wood-concrete beam was measured using the fixture discussed in Chapter 3 and was plotted versus load as shown in Figure 4.8. The behavior of the shear keys is more apparent by enlarging the left-most portion of the plot (see Figure 4.9). From Figure 4.9 it is seen that up to 10 kips of loading, the slip was essentially the same at both ends of the beam, but beyond this load level, the slip was different at each end. Between the 11 kip and 19 kip load levels, the south end slip was higher than that of the north end. Beyond 19 kips, the north end slip was higher than that of the south end.

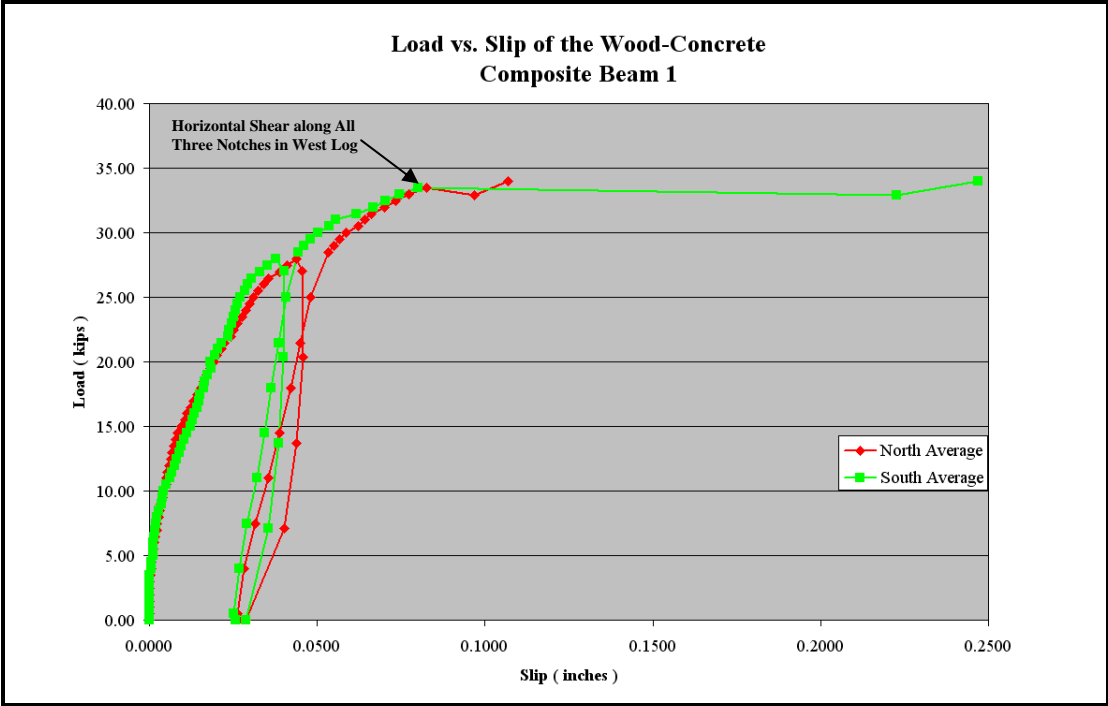


**Figure 4.8** Load vs. Slip for Ultimate Strength Test– Beam 1

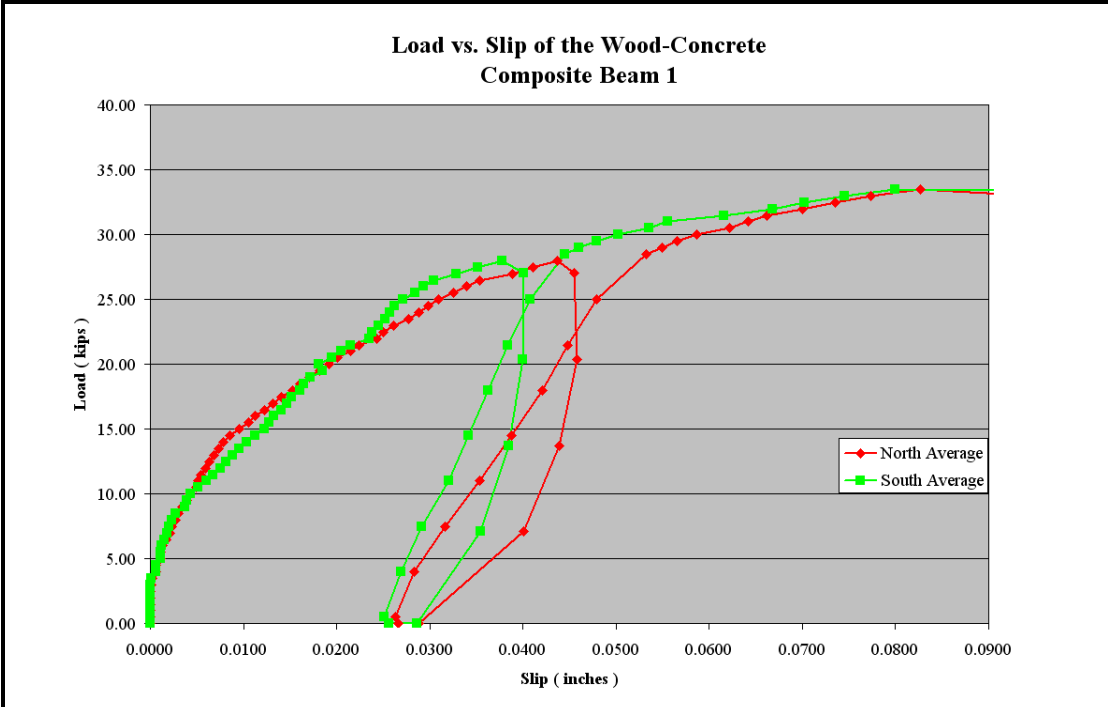


**Figure 4.9** Partial View of Load vs. Slip for Ultimate Strength Test – Beam 1

Beyond 19 kips of loading, the north end slips at a greater rate than the south end. Then at 33.48 kips (see Fig. 4.8), just as the north and south end slips were converging, the shear failure of the west side utility pole occurred, causing the slip on the south side of the beam to jump from 0.0800 inches to 0.2468 inches.

## 4.2 Wood-Concrete Beam 2

The modulus of elasticity of the second beam was determined in a similar manner to the first beam. After the ends were pinned, a single actuator load was applied to the beam at mid span to determine the modulus of elasticity of each utility pole. Again, at this time there were no shear key notches or support notches cut into the utility poles. Figure 4.10 shows the load versus deflection graphs for the mid span deflections of the two utility poles.

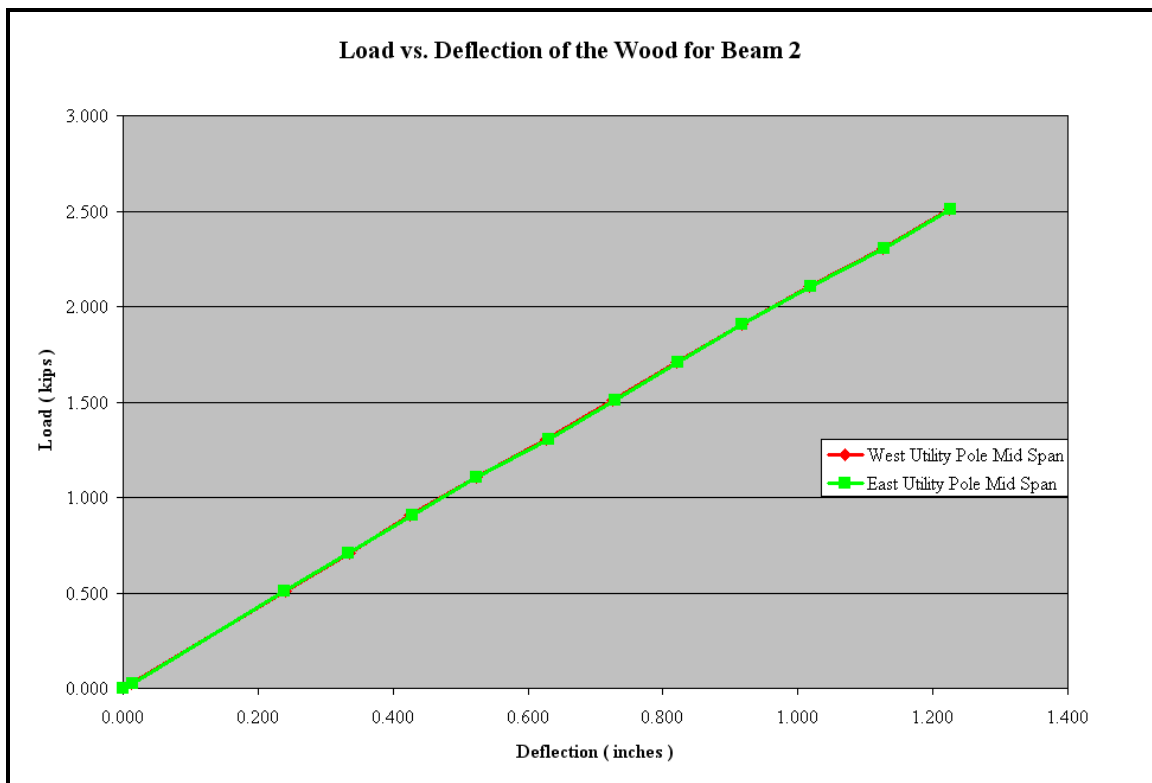


**Figure 4.10** Load vs. Deflection of the Wood – Beam 2

It is evident from Figure 4.10 that the two utility poles have a near equal stiffness. Test cuts on the poles and the initial loading indicated that the two utility poles were made of the same species – Douglas fir. The average modulus of elasticity for the two utility poles was calculated to be 1,966 ksi.

It is evident from Figure 4.11 that between day 17 and day 22 the relative humidity (typically 40% or lower) was high for Fort Collins, Colorado, during the summer. This caused the beam to relax as evident by the increase in the rate of deflection over this period. Yet, when the relative humidity decreased to 40% on the twenty-fourth day, the beam began recovering stiffness. The rebound of the beam from the decrease in humidity was 0.0211 inches.

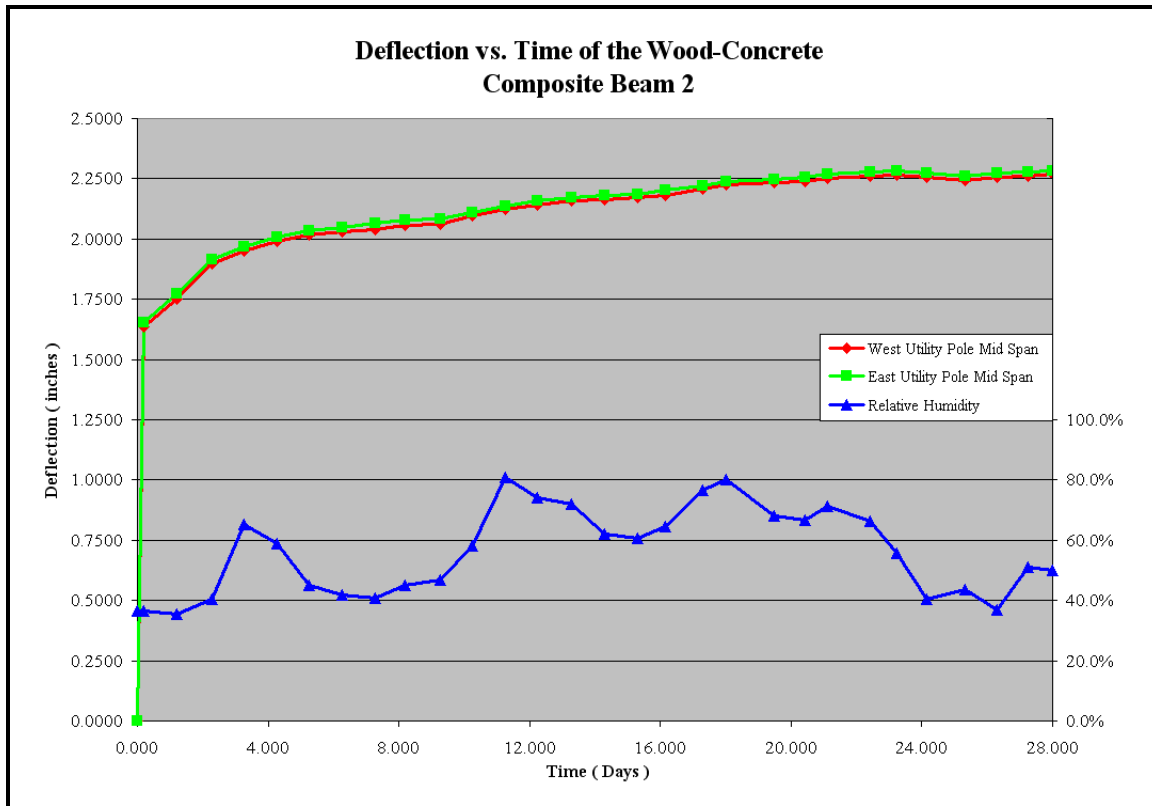


**Figure 4.11** Deflection vs. Time – Beam 2

Wood-Concrete Composite Beam 2 was loaded with a point load at mid span to find its ultimate load capacity using the spreader beam to distribute the load across the width of the beam in the same way as Wood-Concrete Composite Beam 1. Figure 4.12 shows a graph of load versus mid span deflection. The first event that led to a noticeable failure event occurred at a load of 18.98 kips when a mid span flexural crack in the wood of the west utility pole occurred on the tension face near a two-inch knot, causing a small vertical crack. At a load of 27.48 kips, this mid span crack in the west utility pole suddenly grew to three inches in length, and a 14-inch horizontal crack began propagating as shown in Figure 4.13. Once the west utility pole deflected, it placed a higher stress on the east utility pole, causing a small vertical crack to form at mid span.

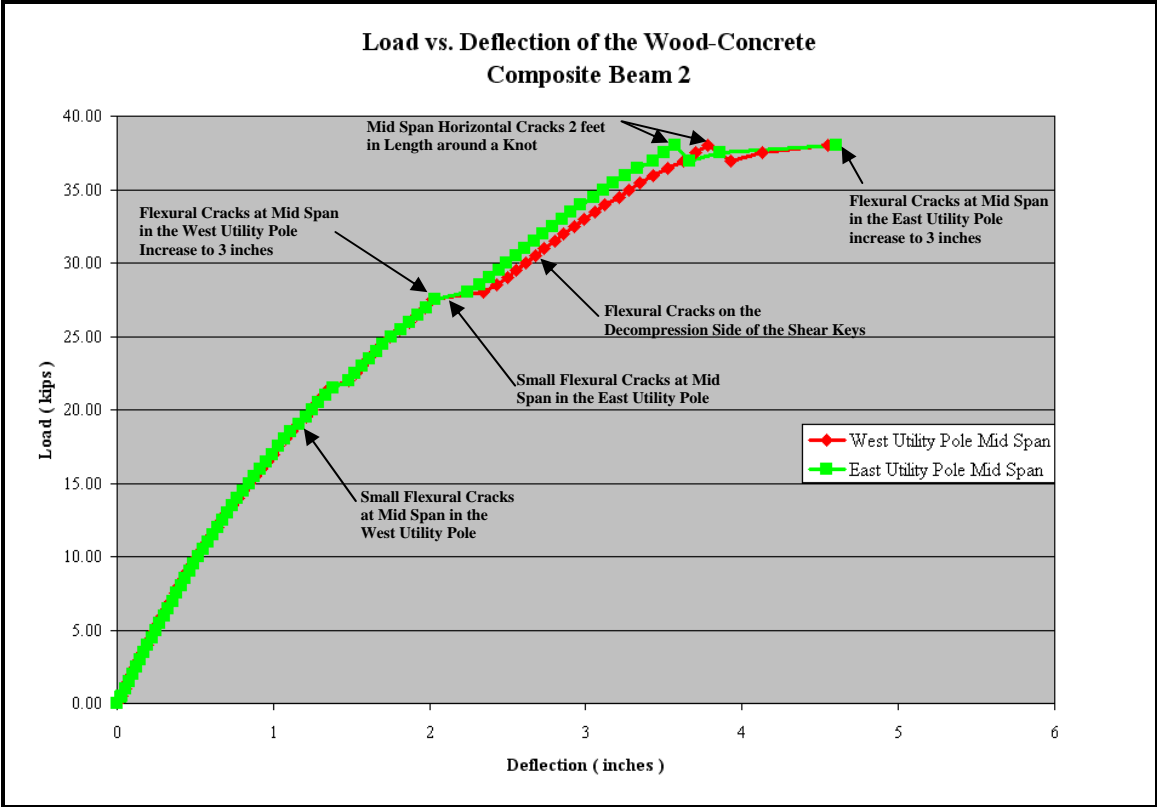


**Figure 4.12** Ultimate Strength Test – Beam 2

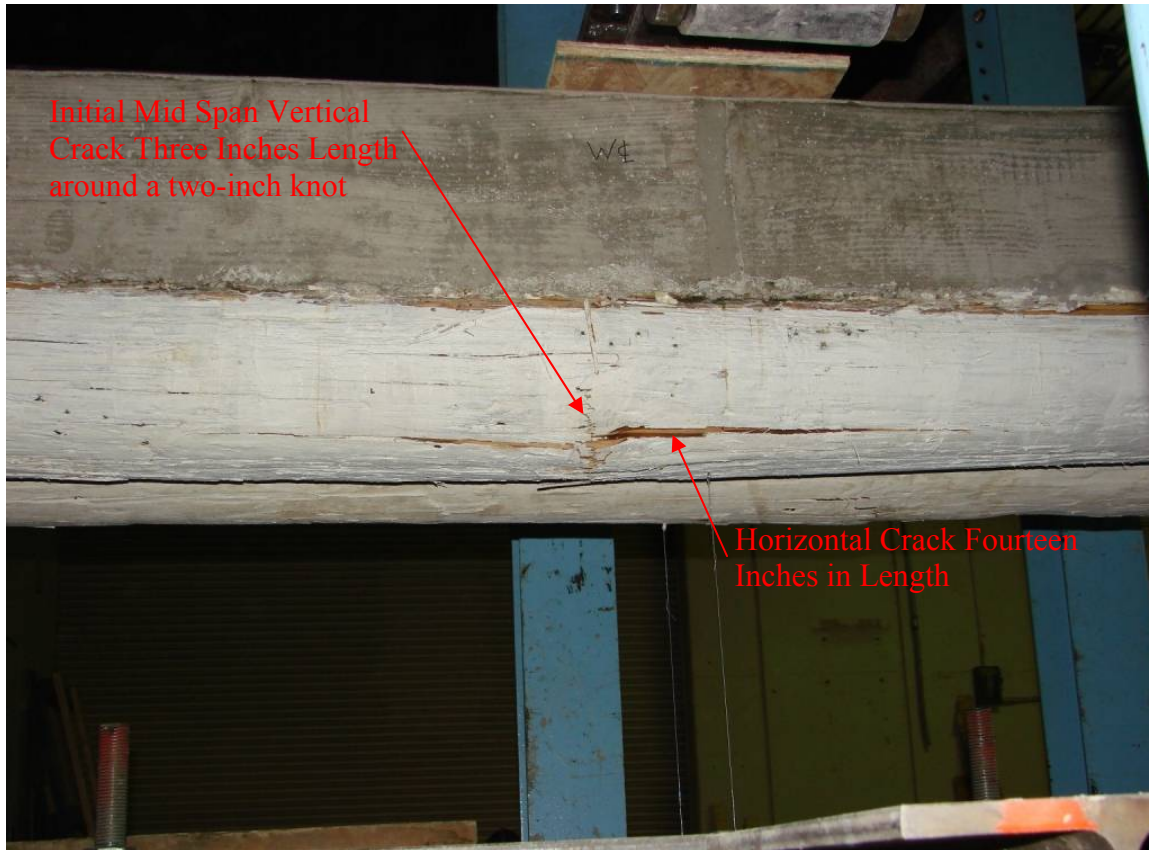


**Figure 4.13** West Side Cracking at Mid Span around a Knot – Beam 2

At 30.48 kips, flexural cracks on the decompression side of the notches began to form as shown in Figure 4.14. The crack shape at all six shear keys was similar. Each crack formed a hooked shape that curved over the base of the notch. The general direction of the forces of the concrete bearing on the wood is drawn in Figure 4.14. In this image, mid span is toward the left of the figure and the south support is toward the right side. At these high loads, vertical cracks at mid span can also be seen (see Figure 4.15). The vertical cracks extended up to the neutral axis of the wood-concrete composite beam.

At 37.55 kips, the high tensile and flexure stress in the wood caused a two-foot horizontal crack at mid span on either side of the vertical crack (see Figure 4.15). These horizontal cracks weakened the specimen, causing 37.55 kips to be the maximum load that the second beam would accept. Additional attempts to apply more load to the beam resulted in an increased deflection of the beam with little increase in load as evident in Figure 4.12. The final failure was a three-inch vertical crack and tear out of the tensile face of the wood as shown in Figure 4.15.

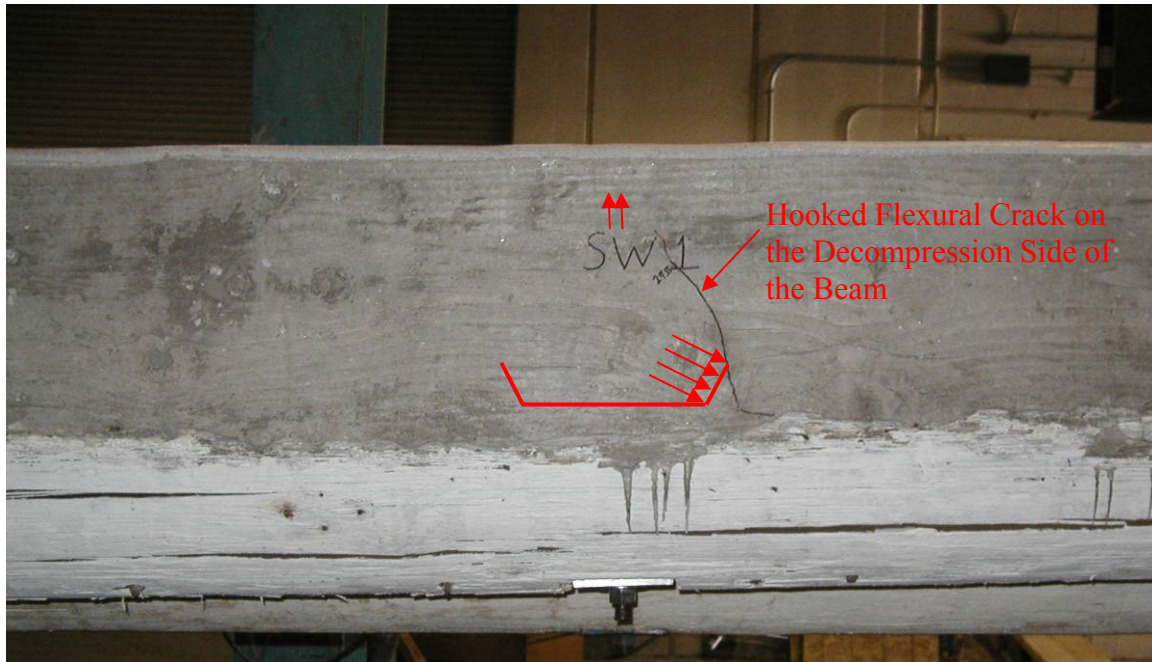


**Figure 4.14** Cracking on the Decompression Side of the Notch – Beam 2

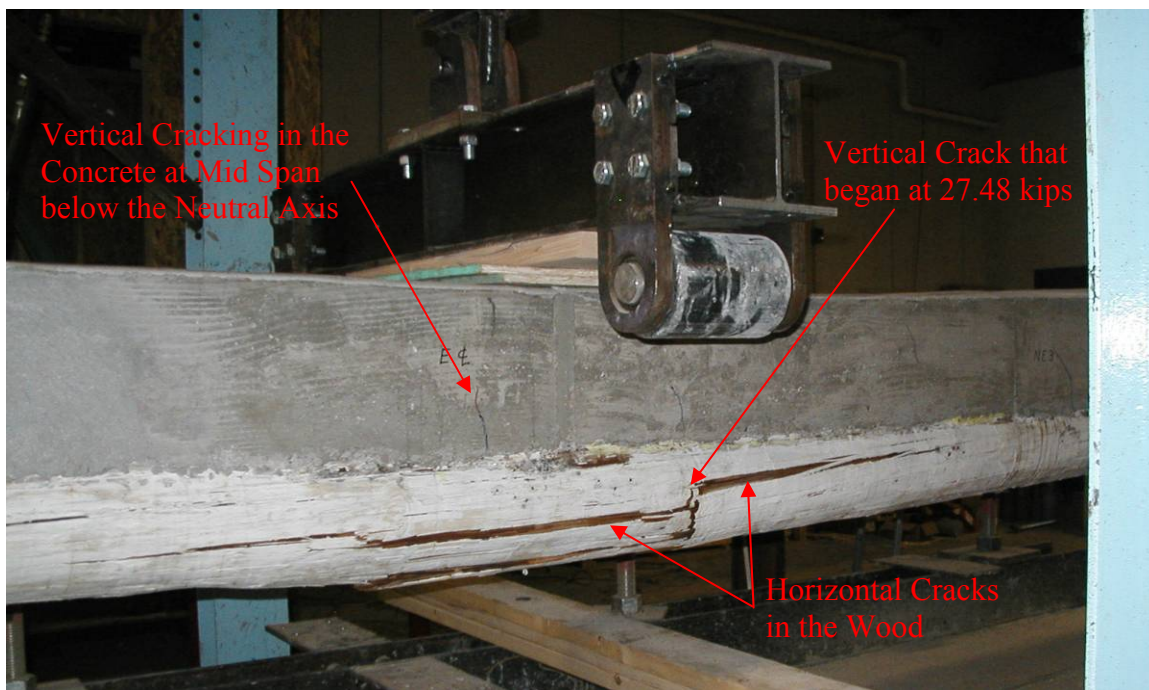


**Figure 4.15** Horizontal Cracks in the East Utility Pole at Mid Span

The slip at each end of the wood-concrete beam was measured using the fixture discussed in Chapter 4 and is plotted versus load in Figure 4.16. For the first five kips of load, the north and south ends slipped evenly. Then the north end of the beam began slipping at a greater rate than the south end. At 26 kips of load, there is a crossover point where both the north and south ends of the beam have a slip of equal value, which is 0.0168 inches. Beyond that load level, the south end exhibited an increase in slip relative

to the north end. It should be noted that the specimen did not exhibit a block shear failure in wood along the notch plane as had occurred in Wood-Concrete Composite Beam 1.



**Figure 4.16** Tear out of the Tension Face – Beam 2

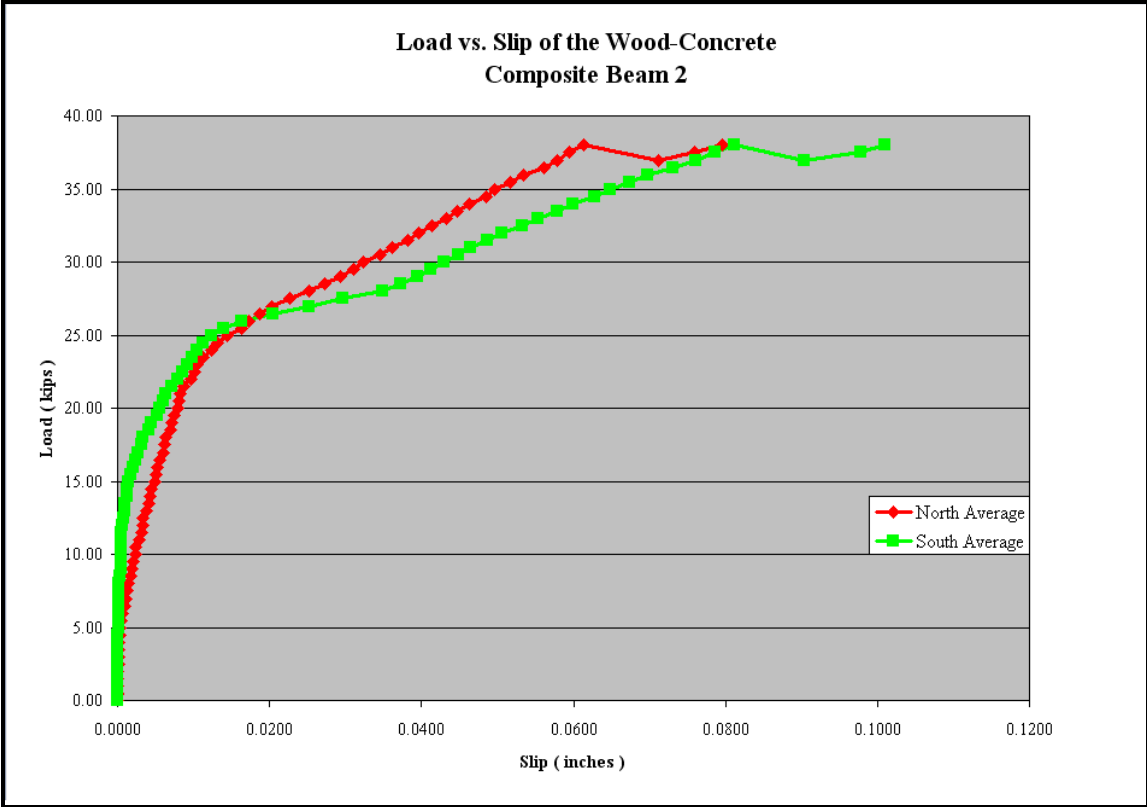


Figure 4.17 Load vs. Slip for Ultimate Strength Test – Beam 2

## 5. DISCUSSION

### 5.1 Time-Dependent Behavior

This section describes a simplified computational procedure developed to predict the deflection of a wood-concrete composite beam over its 28-day curing period. Figure 5.1 shows the data obtained in that period. The trend in relative humidity is also included.

The overall deflection of the beam consists of two effects. The first effect is the initial deflection of the wood utility poles under the weight of the concrete when initially placed atop them. The second event is the time-dependent deflection response over the 28-day curing period. This time-dependent behavior is actually a combination of creep of the two materials, shrinkage, and hygroscopic factors. However, for simplicity, it will be referred to as only “creep.”

In order to predict the total deflection at any point during the curing period,  $\delta_{total}$ , the sum of the two events can be determined from:

$$\delta_{total} = \delta_{initial} + \delta_{creep} \quad \text{Eq. 5.1}$$

Where  $\delta_{initial}$  is the initial deflection from the weight of the concrete, and  $\delta_{creep}$  is the deflection from the multiple time dependent effects.

The value of  $\delta_{initial}$  can be predicted by assuming the weight of the uncured concrete creates a uniform load on the wood utility poles equal to the density of the concrete,  $\rho_c$ , multiplied by the area of untransformed concrete,  $A_c$ , i.e.:

$$\omega_c = \rho_c \cdot A_c \quad \text{Eq. 5.2}$$

The approximate mid span centroidal moment of inertia at mid span of the wood utility poles is:

$$I_w = 2 \cdot \left( \frac{\pi}{4} \right) \cdot \left( \frac{d_w}{2} \right)^4 \quad \text{Eq. 5.3}$$

Where  $d_w$  is the average of mid span diameters of the two poles. As the two poles taper in opposite direction, the average of the two diameters does not change much over the length of the specimen. Consequently,  $\delta_{initial}$  is approximately:

$$\delta_{initial} = \frac{5 \cdot \omega_c \cdot L^4}{384 \cdot E_w \cdot I_w} \quad \text{Eq. 5.4}$$

The second effect (the “creep”) is modeled by fitting an empirical equation to the actual data collected from the time of initial deflection to the 28<sup>th</sup> day of curing (see Fig. 5.1).

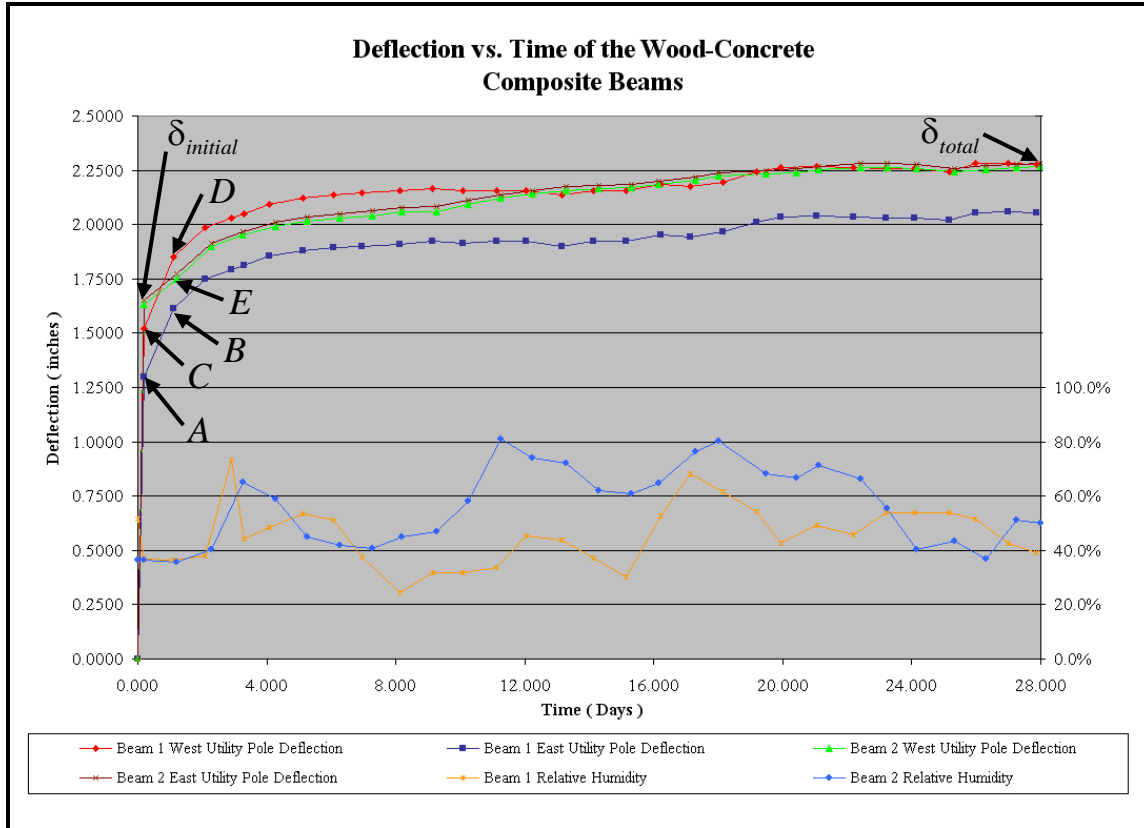


**Figure 5.1** Mid Span Deflection versus Time for Wood-Concrete Composite Beams 1 and 2

The creep deflection of the beam,  $\delta_{creep}$ , is defined as:

$$\delta_{creep} = \delta_{total} - \delta_{initial} \quad \text{Eq. 5.5}$$

Where  $\delta_{initial}$  is the initial measured deflection of the beam due to the weight of the wet concrete and  $\delta_{total}$  is the total deflection of the beam from that effect plus the creep effects.

In order to fit an empirical equation to the data that is representative of the creep the beam experiences between the 1<sup>st</sup> and 28<sup>th</sup> days, the portion of the data after the initial deflection of the beam needs to be isolated. However, in Fig. 5.1 it is evident that the east utility pole of Wood-Concrete Composite Beam 1 experienced an additional high deflection between point A and point B. Similarly, the west utility pole experienced a high deflection between point C and point D. A possible reason for these high deflections is that the wood forms used to restrain the concrete as it was placed on top of the utility poles were of substantial size relative to the wood utility poles (see Figure 3.14). In the case of Wood-Concrete Composite Beam 1, the forms were physically attached to the wood utility poles. Due to their size and connection with the utility poles, they increased the moment of inertia and added stiffness to the beam. When the forms were removed, sometime between measurements A and B for the east pole and between points C and D for the west pole, the beam lost the additional moment of inertia from the forms and resumed its “natural” deflection. A vertical jump in deflection likely occurred when the forms were removed, but this jump was not captured by the data acquisition system due to the discrete time increments used. In contrast, the forms were installed on Wood-Concrete Composite Beam 2 so that they were loose relative to the utility poles and incapable of increasing the moment of inertia of specimen.

Recall that the two utility poles of Wood-Concrete Composite Beam 1 were of different species, which is primarily why they had different initial deflections. Once the concrete layer hardened enough, the resulting rigidity of the layer constrained the two utility poles to deflect in unison. Therefore, to account for that condition, the graph of the west utility pole was shifted downward toward the graph of the east utility pole so that points B and D coincide. Then the coincident points B and D of Fig. 5.1 were shifted up to point E of Fig. 5.1. The resulting point is the datum for the deflection versus time graphs shown in Figure 5.2. The reason for not using  $\delta_{initial}$  (i.e., point A of Fig. 5.1) as the datum in Fig. 5.2 is to remove the effect of the load sharing of the forms in Wood-Concrete Beam 1.

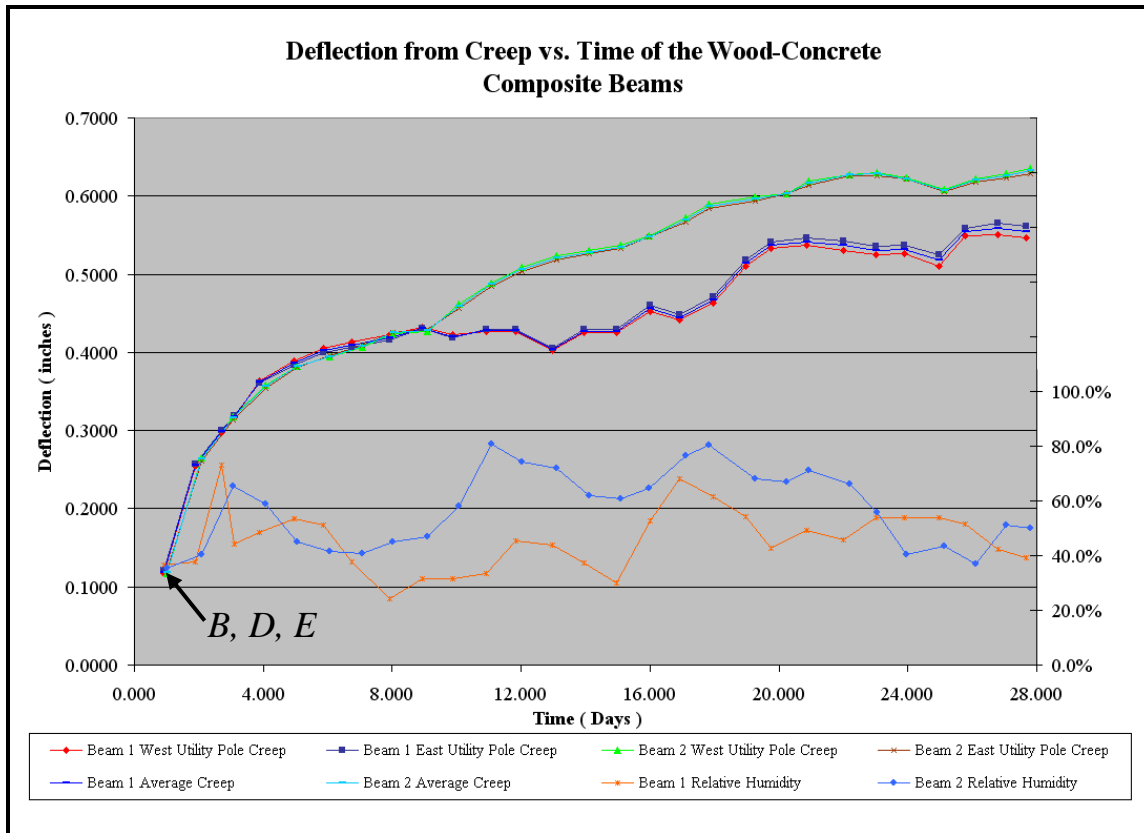


**Figure 5.2** Mid-Span Deflection from Creep versus Time

In addition to the individual measured mid span deflection due to creep of each of the two utility poles of each composite beam specimen, Fig 5.2 also includes the average mid span creep of each specimen. This plot of the average creep was used as a basis to fit a natural logarithm trend line to the creep data. The plots of average creep of each specimen were fitted with a logarithmic trend line. The trend line based on data of Wood-Concrete Composite Beam 2 had a higher  $R^2$  value of 0.985 versus the  $R^2$  value of 0.924 for Wood-Concrete Composite Beam 1. Wood-Concrete Composite Beam 2 also had a higher creep over the 28-day period and, hence, provides an upper bound mid span deflection estimate. Therefore, the mid span deflection data of Wood-Concrete Composite Beam 2 was used to generate an empirical creep equation for mid span deflection due to creep  $\delta_{emp\_creep}$ .

The trend line fitted to Wood-Concrete Beam 2 is shown in Figure 5.3. The resulting empirical expression for  $\delta_{emp\_creep}$  as a function of time is:

$$\delta_{emp\_creep} = 0.1544 \cdot \ln(t) + 0.12486 \quad \text{Eq. 5.6}$$

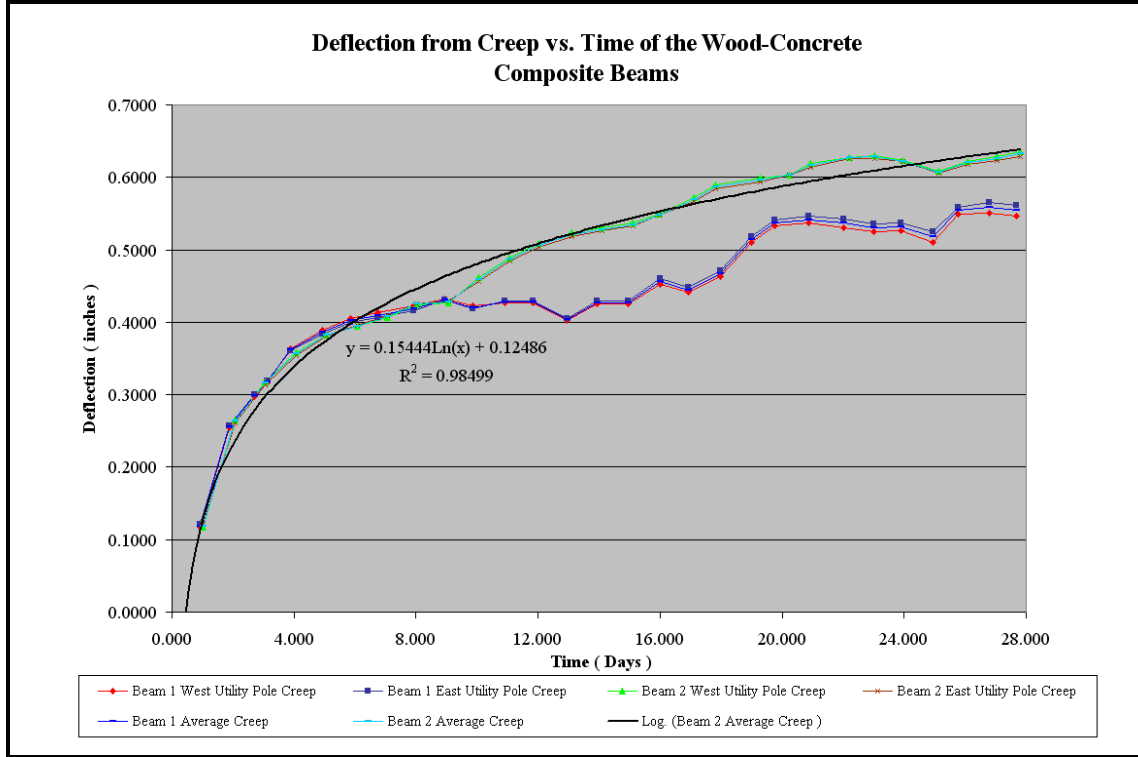


**Figure 5.3** Deflection from Creep versus Time with a Trend Line

Eq. 5.6 applies only to this particular beam configuration. What is needed is a way to predict creep as a function of time for a wood-concrete beam made of utility poles with different combinations of fully composite moment of inertia, span, initial concrete load, moment of inertia of the wood only, and modulus of elasticity of the wood. To accomplish this the expression for deflection due to creep, Eq. 5.6 can be equated to the deflection equation for a simply supported beam with a uniform load and solved for an equivalent load due to creep as a function of time. This would simulate the effect of creep as uniform load,  $\omega_{creep}$ , increasing as a function of time. This concept is developed as follows:

$$\delta_{emp\_creep} = \frac{5 \cdot \omega_{creep} \cdot L_2^4}{384 \cdot E_{w2} \cdot \bar{I}_2} \quad \text{Eq. 5.7}$$

Substitution Eq. 5.6 and solving for  $\omega_{creep}$  yields:

$$0.1544 \cdot \ln(t) + 0.12486 = \frac{5 \cdot \omega_{creep} \cdot L_2^4}{384 \cdot E_{w2} \cdot \bar{I}_2}$$

$$\omega_{creep} = \frac{E_{w2} \cdot \bar{I}_2 \cdot (11.85792 \cdot \ln(t) + 9.589248)}{L_2^4} \quad \text{Eq. 5.8}$$

It is important to note that Eq. 5.7 is the equivalent uniform load for creep based on the section and material properties of Wood-Concrete Composite Beam 2. Table 5.1 lists selected properties of the two wood-concrete composite beams tested. To establish the simulated load corresponding to the creep deflection, substitute the cross-sectional properties into Eq. 5.7.

**Table 5.1** Selected Beam Properties for Creep

	Wood-Concrete Beam 1	Wood-Concrete Beam 2
Density of Concrete	$\rho_{c1} = 0.150 \text{ kips/ft}^3$	$\rho_{c2} = 0.150 \text{ kips/ft}^3$
Area of the Concrete	$A_{c1} = 172.76 \text{ in}^2$	$A_{c2} = 181.46 \text{ in}^2$
Span Length	$L_1 = 354.24 \text{ in}$	$L_2 = 354.24 \text{ in}$
Fully Composite Moment of Inertia	$\bar{I}_1 = 16084.38 \text{ in}^4$	$\bar{I}_2 = 11348.65 \text{ in}^4$
Modulus of Elasticity for the Wood	$E_{w1} = 1.1065 \cdot 10^6 \text{ psi}$	$E_{w2} = 1.966 \cdot 10^6 \text{ psi}$
Moment of Inertia of the Wood Utility Poles	$\bar{I}_{w1} = 1952.25 \text{ in}^4$	$\bar{I}_{w2} = 981.75 \text{ in}^4$
Weight of the Concrete	$\omega_{c1} = 15.0 \text{ lbs/in}$	$\omega_{c2} = 15.752 \text{ lbs/in}$

Using the cross-sectional properties of Wood-Concrete Beam 2 provided in Table 5.1, the simulated uniform creep load is obtained by:

$$\omega_{creep} = \frac{1.966 \cdot 10^6 \cdot 11348.65 \cdot (11.85792 \cdot \ln(t) + 9.589248)}{354.24^4}$$

$$\omega_{creep} = 16.80141 \cdot \ln(t) + 13.58695 \quad \text{Eq. 5.9}$$

Eq. 5.9 is then be substituted into the deflection equation for a simply supported beam to find the generalized equation for mid span deflection due to creep,  $\delta_{creep}$ , as shown below:

$$\delta_{creep} = \frac{5 \cdot \omega_{creep} \cdot L^4}{384 \cdot E_w \cdot \bar{I}}$$

$$\delta_{creep} = \frac{5 \cdot [16.8014 \cdot \ln(t) + 13.5869] \cdot L^4}{384 \cdot E_w \cdot \bar{I}} \quad \text{Eq. 5.10}$$

The total deflection of the wood-concrete beam can be predicted by adding the initial deflection due to the concrete weight (Eq. 5.3) and the deflection due to the creep given (Eq. 5.10) as shown below:

$$\delta_{total} = \delta_{initial} + \delta_{creep}$$

$$\delta_{total} = \frac{5 \cdot \omega_c \cdot L^4}{384 \cdot E_w \cdot I_w} + \frac{5 \cdot [16.8014 \cdot \ln(t) + 13.5869] \cdot L^4}{384 \cdot E_w \cdot \bar{I}} \quad \text{Eq. 5.11}$$

Where  $t \leq 28$  days

Using Eq. 5.11, it is possible to predict the total deflection resulting after the 28-day curing period. A sample calculation (for the 28<sup>th</sup> day outcome) using the data for Wood-Concrete Beam 1 given in Table 5.1 is shown below:

$$\delta_{total1} = \frac{5 \cdot 15 \cdot 354.24^4}{384 \cdot 1.1065 \cdot 10^6 \cdot 1952.75} + \frac{5 \cdot [16.8014 \cdot \ln(28) + 13.5869] \cdot 354.24^4}{384 \cdot 1.1065 \cdot 10^6 \cdot 16084.38}$$

$$\delta_{total1} = 2.225 \text{ in}$$

The predicted average wood-concrete composite deflection as a function of time and the average measured deflection of each of the two wood-concrete composite beams are shown in Figure 5.4. From Figure 5.4, it is evident that the actual measured average mid span deflection of the two utility poles comprising each wood-concrete composite beam closely follow the predicted creep and deflection from the initial concrete load.

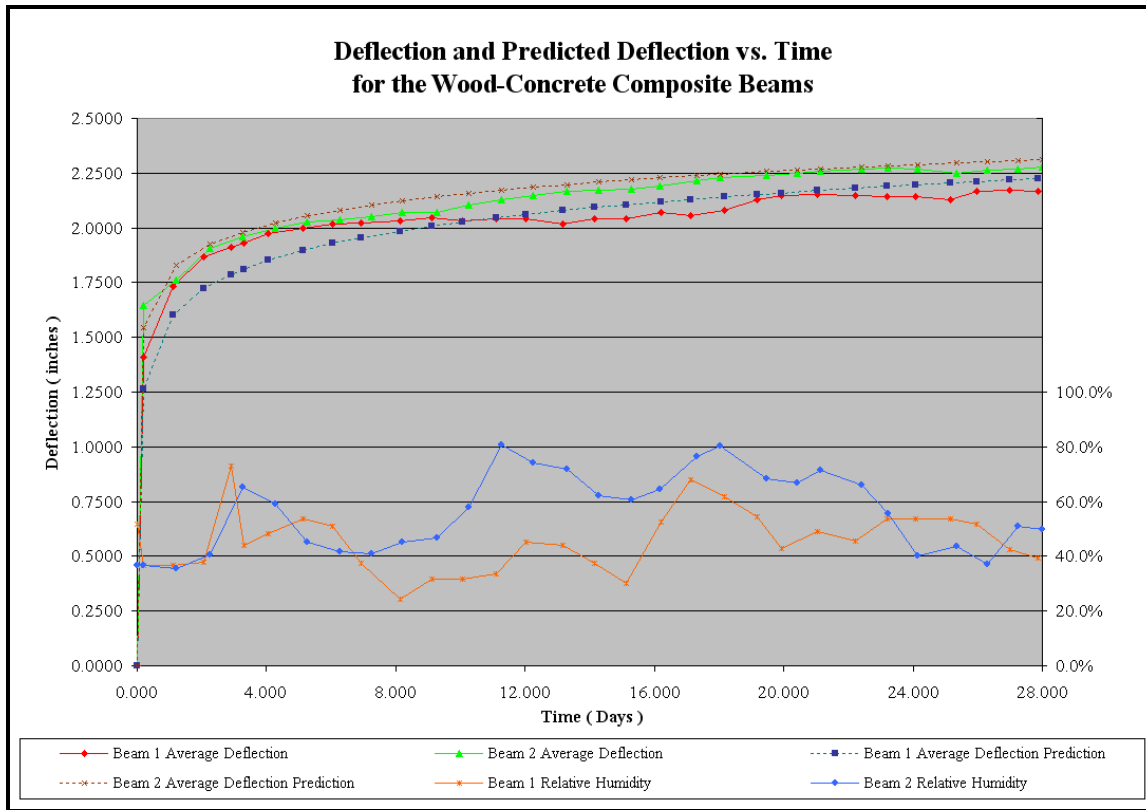


**Figure 5.4** Predicted Deflection for the Wood-Concrete Beams

The percent error between the theoretically predicted deflection and the experimental deflection is quantified as follows:

$$\%Error = \frac{|Theoretical-Experimental|}{Theoretical} \cdot 100$$

The trends in percent error (between the predicted and experimental deflection over the 28-day period) versus time for the two wood-concrete composite beams are plotted in Figure 5.5.

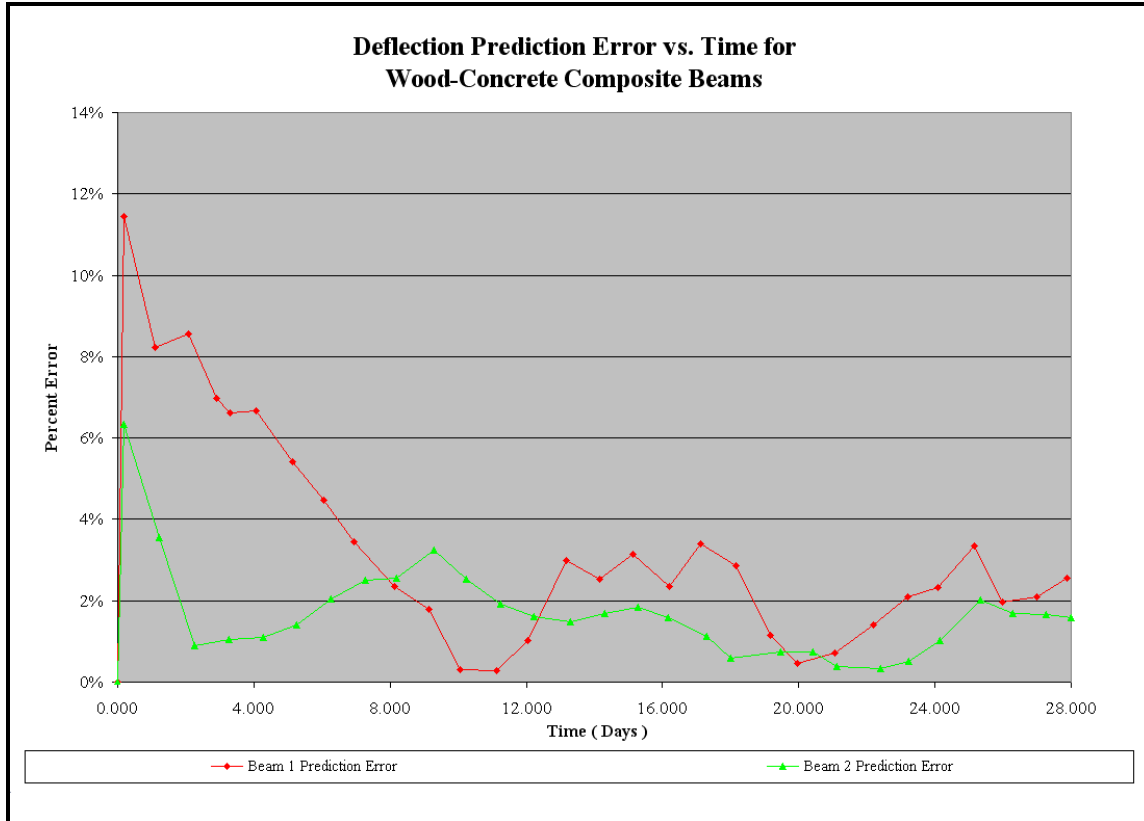


**Figure 5.5** Percent Error between the Average and Predicted Beam Deflections

For Wood-Concrete Composite Beam 1, the initial deflection was under predicted by 11.5%, i.e., by 0.145 inches. However, beyond the seventh day the percent error falls below 3.5%, which corresponds to under predicting the deflection by  $\frac{1}{16}$ <sup>th</sup> of an inch. The initial deflection for Wood-Concrete Composite Beam 2 was under predicted by 6.3%, but after the first day, the predicted deflection was within 3.5% of the beam's actual deflection over a 28-day period.

## 5.2 Design Method Verification

For practical use, the observed ultimate capacity should be compared to a code-based design load requirement. For a structure to be mechanically adequate, the load capacity of the structure must be greater than or equal to the expected demand. Wood is a natural product and hence has variability in its mechanical properties. If a sample was taken from a group of boards and a particular property was measured, a normal probability distribution would be created<sup>15</sup> as shown qualitatively in Figure 5.6.

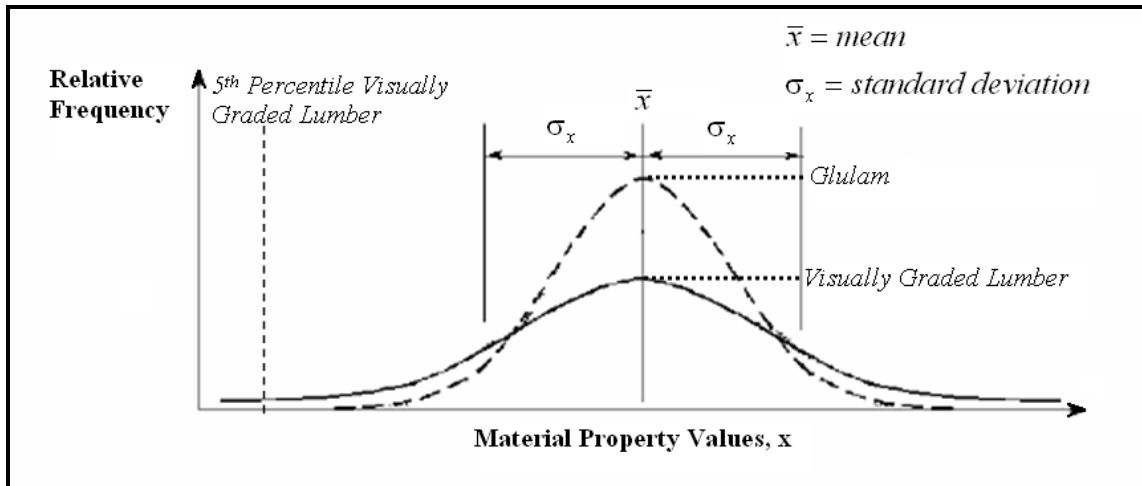


**Figure 5.6** Material Property Distribution<sup>26</sup>

Figure 5.6 illustrates the qualitative material property distributions for glue-laminated lumber and visually graded lumber. The distribution for glue-laminated lumber is tighter with less variability since it is a manufactured wood product using tightly graded material. In contrast, visually graded lumber has a broader stress distribution, which indicates increased variability in the natural material. A utility pole would likely be in between these distributions. To account for this variability, the reference design values in the NDS are calculated using the material properties found below the 5<sup>th</sup> percentile.

Figure 5.7 illustrates the qualitative load and resistance distributions plots. There is an overlap, shown in shading, between the load and resistance distribution where load level might exceed the resistance level. Subtracting the load distribution from the resistance distribution yields the performance distribution shown in Figure 5.8. The performance values which fall below the reliability index ( $\beta$ ) multiplied by one standard deviation are considered a failure for design purposes. To minimize the number of performance values that are less than the quantity  $\beta \cdot \sigma_z$ , while still maintaining an economically feasible structure, the reliability index typically is set between 5.6 and 5.9.<sup>26</sup>

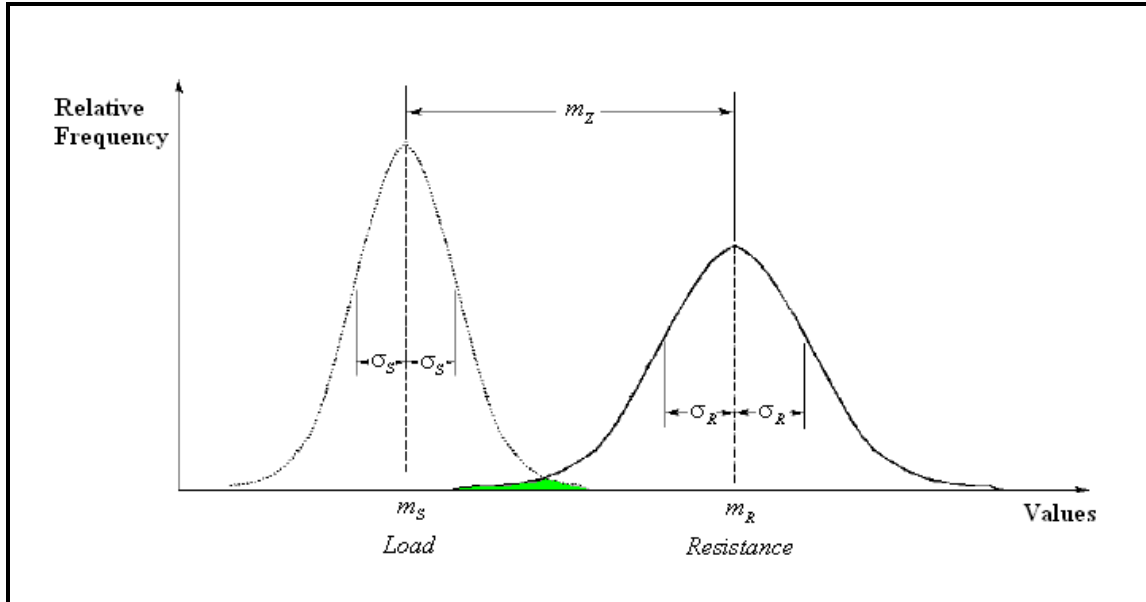


Figure 5.7 Sample Distributions of Load and Resistance<sup>26</sup>

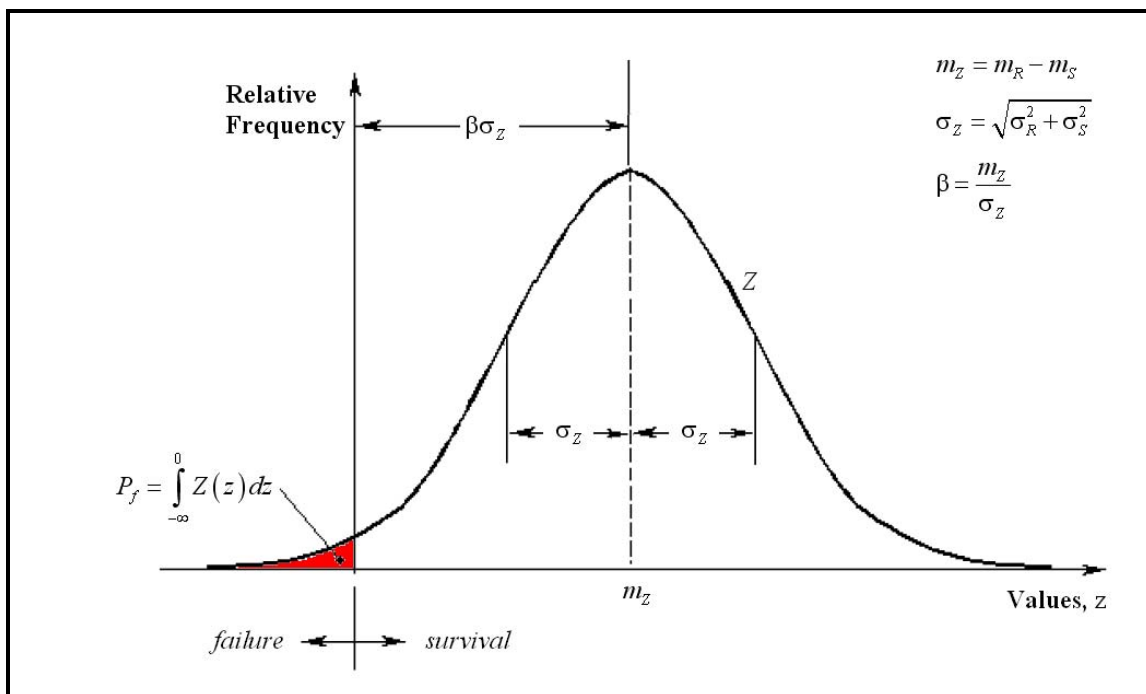


Figure 5.8 Performance Distribution<sup>26</sup>

A design method presented in the thesis work on this project<sup>18</sup> predicted that the maximum factored load that could be applied to the wood-concrete composite beam was limited by the combined bending and axial stresses at the inner notch. The ultimate load tests of the wood-concrete composite beams presented in Chapter 5 of this report showed that both beam specimens had failures from a combination of bending and tension in the wood. This confirmed a predicted outcome obtained using the potential design procedure.<sup>19</sup> Therefore, when assessing the reliability of the structure, the wood controls the reliability of the wood-concrete composite beam.

The performance of the wood-concrete composite beam can be quantified by:

$$z = R - S \quad \text{Eq. 5.12}$$

Where  $z$  is the performance value of the wood-concrete composite beam,  $R$  is the resistance of the beam from the ultimate load test, and  $S$  is the factored load from the design method. To create a resistance distribution with a 75% confidence interval for calculating the performance distribution, a minimum of 28 samples are needed.<sup>16</sup> Yet, the NDS already has  $\beta\sigma_z$  built into the load factors, resistance factors, and reference design values so that when a wood structure is designed, the difference between the load and resistance values will be greater than  $m_z$ , i.e., is the mean value of the probability distribution.

As a comparison to the wood-concrete beam test data shown in Chapter 4, it would be informative to know the ultimate capacity of the wood-concrete composite beam if the utility poles used in the beams' construction had material properties at the average of the 5% exclusion limit. The bending and tensile stresses at rupture for various types of wood species at the 5% exclusion limit can be found by using the procedures set forth by the American Society for Testing and Materials (ASTM). The ASTM D245-06<sup>17</sup> specification describes how to modify the reference design stresses in the NDS to determine the stresses at rupture. To find the ultimate load based on the 5% exclusion limit using ASTM D245-06, the reference design values for tension and bending given in the NDS are multiplied by an adjustment factor of 2.1. This factor changes the reference design values to the mean ultimate strength of the wood below the fifth percentile.

To determine the ultimate load of a wood-concrete beam constructed using utility poles that had material properties at the wood's mean strength or  $\bar{x}$  as shown in Figure 5.6, the specifications in ASTM D245-06 are used. This standard specifies how to adjust the average clear wood stress for a species of wood based on the defects present within the wood. Defects that reduce the flexural and tensile capacity of the wood include knots and slope of grain, among other lesser factors. There are tables within ASTM D245-06 that show by what percentage the average clear wood strength is reduced by certain amounts, depending on the nature of the defect. The clear wood strength values used in the calculations are provided in ASTM D2555-06.<sup>18</sup>

The load versus deflection graph for the first wood-concrete composite beam is shown in Figure 5.9. In addition to the mid span deflections of the two utility poles used in the wood-concrete composite beam, the idealized (computed) fully composite and non-composite deflections based on the geometry of Wood-Concrete Composite Beam 1 are plotted for reference. It can be seen that the service load capacity for that specimen is 9.72 kips as predicted from the design method<sup>18</sup> using the weaker of the two species, which is western red cedar. For more information on calculating the design and factored loads, the reader is referred to the design method presented by LeBorgne.<sup>19</sup> The factored load is determined by multiplying the service load by the live load factor of 1.6, which gives a factored load of 15.55 kips. Using the ultimate tension and flexural stresses for wood at the fifth percentile, the ultimate load for the wood-concrete composite beam is determined to be 19.80 kips. Then, using the average clear wood modulus of rupture stress values for western red cedar multiplied by a 0.75 strength ratio for a 2-inch diameter knot at mid span on the tension face of the cedar utility pole, the ultimate load is determined to be 32.52 kips.

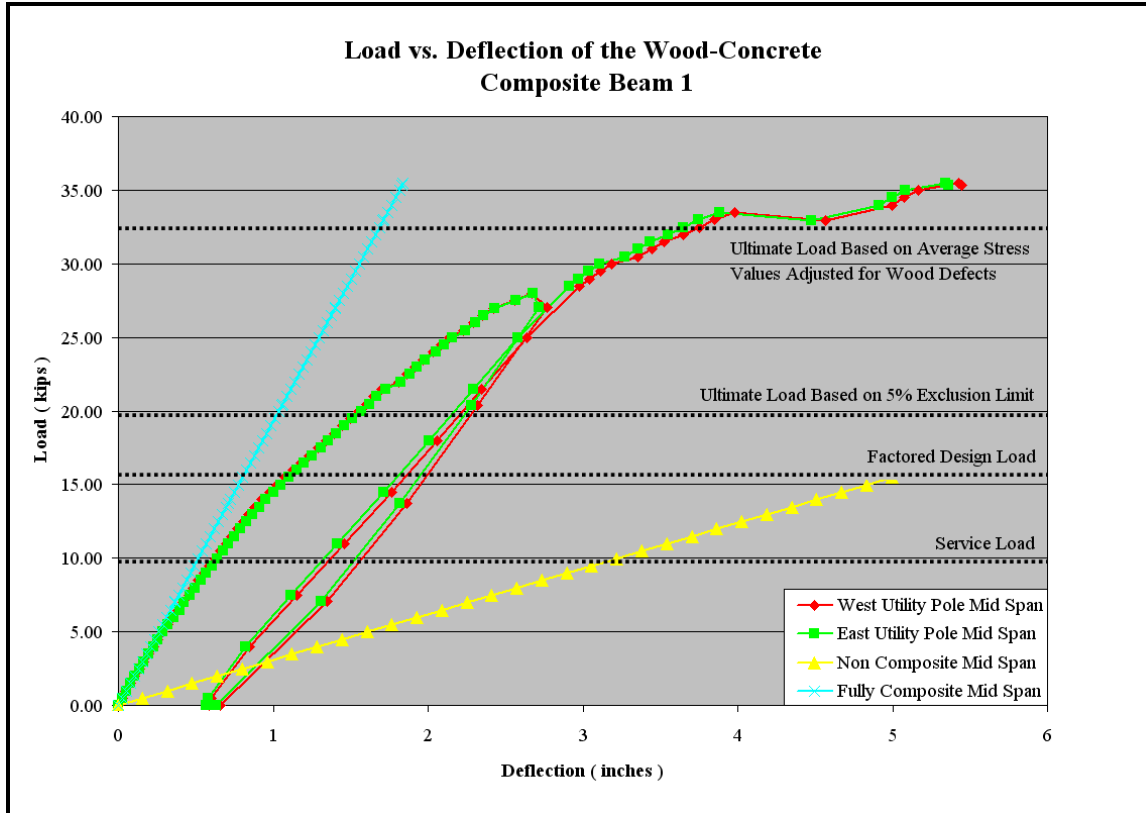


**Figure 5.9** Ultimate Loads for Wood-Concrete Composite Beam 1

The plot shown in Figure 5.9 indicates that Wood-Concrete Composite Beam 1 has an ultimate load,  $P_{ultimate} = 35.48$  kips, which is 2.96 kips above the clear wood mean ultimate load corrected for defects in the wood,  $P_{\bar{x}}$ . Additionally, the ultimate load based upon the 5% exclusion limit,  $P_{5\%} = 19.80$  kips is 15.68 kips below the ultimate strength of Wood-Concrete Composite Beam 1. The factored design load of  $P_u = 15.55$  kips is 19.93 kips below the ultimate strength. The service load of  $P_a = 9.72$  kips is 25.76 kips below the ultimate strength of the Wood-Concrete Composite Beam 1. This suggests that the utility poles used to design Wood-Concrete Composite Beam 1 were near the average strength of the applicable wood species.

The load versus deflection graph for Wood-Concrete Composite Beam 2 was shown earlier in Figure 5.10. In addition to the mid span deflections of the two utility poles used in that specimen, the idealized fully composite and non-composite deflections based on the geometry of that beam one were plotted for reference. Consequently, from Fig. 5.10, it is evident that the service load capacity for Wood-Concrete Composite Beam 1 is 12.22 kips, as predicted from the envisioned design method using reference design values for Douglas fir. Multiplying the service load by the live load factor of 1.6 yields a factored load of 19.55 kips. Using the ultimate tension and flexural stresses for wood at the fifth percentile, the ultimate load for the wood-concrete composite beam was found to be 24.64 kips. Then, using the average clear wood modulus of rupture stress values for Douglas fir multiplied by a 0.75 strength ratio for a 2-inch knot at mid span on the tension face of the west utility pole, the ultimate load is 33.63 kips.

The plot shown in Figure 5.10 indicates that the Wood-Concrete Composite Beam 2 has an ultimate load of  $P_{ultimate} = 37.98$  kips, which is 4.35 kips above the clear wood mean ultimate load corrected for defects in the wood ( $P_{\bar{x}}$ ). Additionally, the ultimate load based upon the 5% exclusion limit of  $P_{5\%} = 24.64$  kips is 13.34 kips below the ultimate strength of Wood-Concrete Composite Beam 2. The factored design load of  $P_u = 19.55$  kips is 18.43 kips below the ultimate strength of the beam, and the service load of  $P_a = 12.22$  kips is 25.76 kips below the ultimate strength of the Wood-Concrete Composite Beam 2. This shows that the utility poles used to design Wood-Concrete Composite Beam 2 were near the average strength of the wood's species. The data for the two wood-concrete composite beams are summarized in Table 5.2.

**Table 5.2** Summary of Wood-Concrete Composite Beam Loads

	$P_a$	$P_u$	$P_{5\%}$	$P_{\bar{x}}$	$P_{ultimate}$
	Allowable Service	Ultimate Design	5% Exclusion	Adjusted Clear	Beam Ultimate
	( kips )	( kips )	( kips )	( kips )	( kips )
Beam 1	9.72	15.55	19.8	35.52	35.48
Beam 2	12.22	19.55	24.64	33.63	37.98

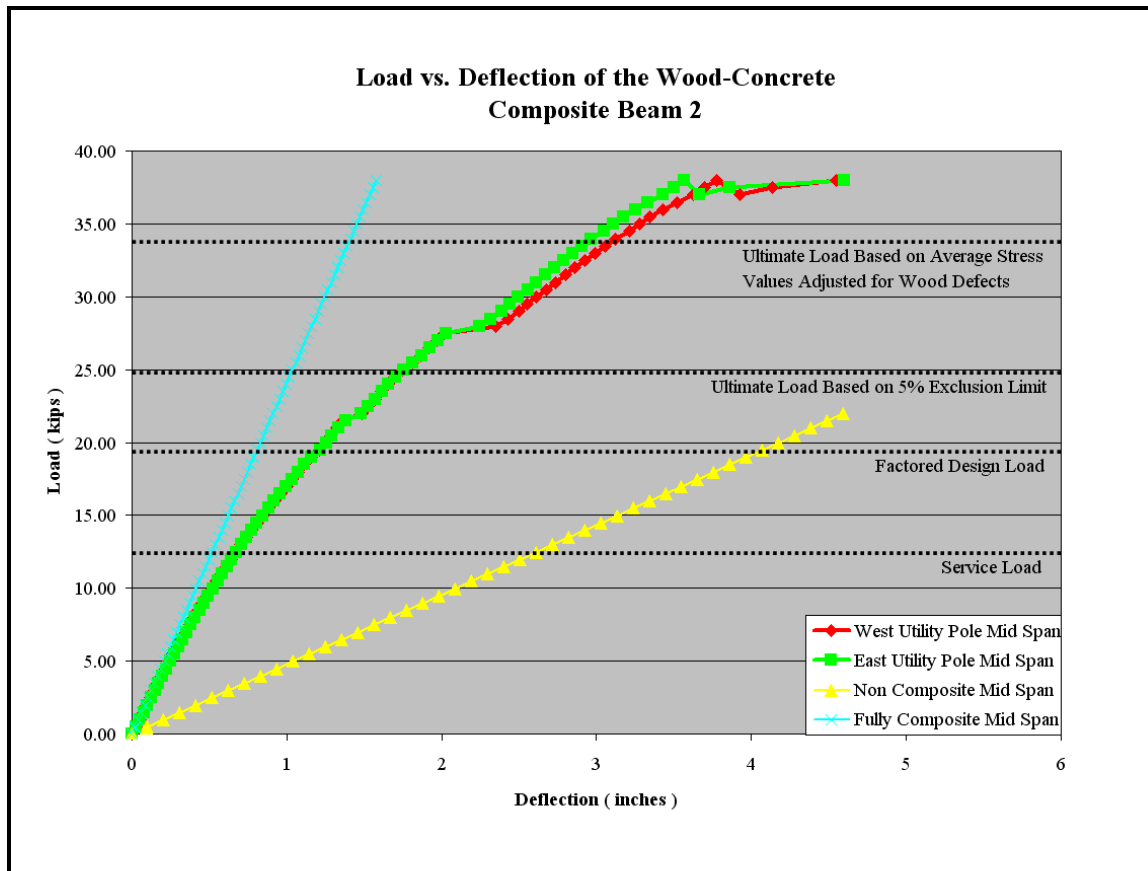


**Figure 5.10** Ultimate Loads for Wood-Concrete Composite Beam 2

Table 5.3 summarizes the difference between the ultimate load and each load state. The envisioned design method provides nearly the same margin between ultimate load and the service load even though Wood-Concrete Composite Beams 1 and 2 utilized different sectional properties, wood species, and concrete compressive stresses. This shows that the design method can adequately predict the service load capacity of the wood-concrete composite beams tested in this study.

**Table 5.3** Summary of Load Margin for the Wood-Concrete Composite Beam

	$P_{ultimate} - P_a$	$P_{ultimate} - P_u$	$P_{ultimate} - P_{5\%}$	$P_{ultimate} - P_{\bar{x}}$
	( kips )	( kips )	( kips )	( kips )
Beam 1	25.762	19.931	15.679	2.958
Beam 2	25.763	18.432	13.345	4.350

### 5.3 Efficiency

The design procedure proposed by LeBorgne<sup>19</sup> is based on an assumption of full composite action existing and then uses a reduction factor to account for the additional mid span stresses induced by partially composite action. As the efficiency decreases, there is greater slip between the wood and concrete layer, which causes increased flexural stresses in the wood. The composite efficiency of a wood-concrete beam composed of utility poles can be calculated using the efficiency equation described by Pault<sup>11</sup>:

$$EFF_{s1} = \frac{\Delta_N - \Delta_P}{\Delta_N - \Delta_C} \quad \text{Eq 0.2}$$

Where  $\Delta_N$  is the theoretical non-composite deflection,  $\Delta_P$  is the measured partially composite deflection, and  $\Delta_C$  is the theoretical fully composite deflection. Equation 5.12 quantifies the effect illustrated in Figure 2.4, as described by Pault.<sup>11</sup>

Like all beams, the wood-concrete-composite beam will generally see the majority of its loads below the service load capacity. Therefore, when fitting trend lines, only the data below the service load capacity is used to calculate the beam's efficiency. Using the trend line fitted to the west utility pole deflection data for the first beam, the average slope of the data is as shown in Figure 5.11. Using the service load of 9.72 kips, the partially composite deflection can be found by dividing 9.72 by the slope of the trend line, which is 16.23. This equals an average deflection of 0.599 inches. Assuming that the beam is fully composite, the deflection at a load of 9.72 kips is 0.504 inches. Similarly, if the beam is non-composite, the deflection at a load of 9.72 kips is 3.136 inches. Using Equation 5.12, the resulting composite efficiency of Wood-Concrete Composite Beam 1 in the service load range is obtained as:

$$EFF_{s1} = \frac{\Delta_N - \Delta_P}{\Delta_N - \Delta_C} \rightarrow EFF_{s1} = \frac{3.136 - 0.599}{3.136 - 0.504} \rightarrow EFF_{s1} = 96.4\%$$

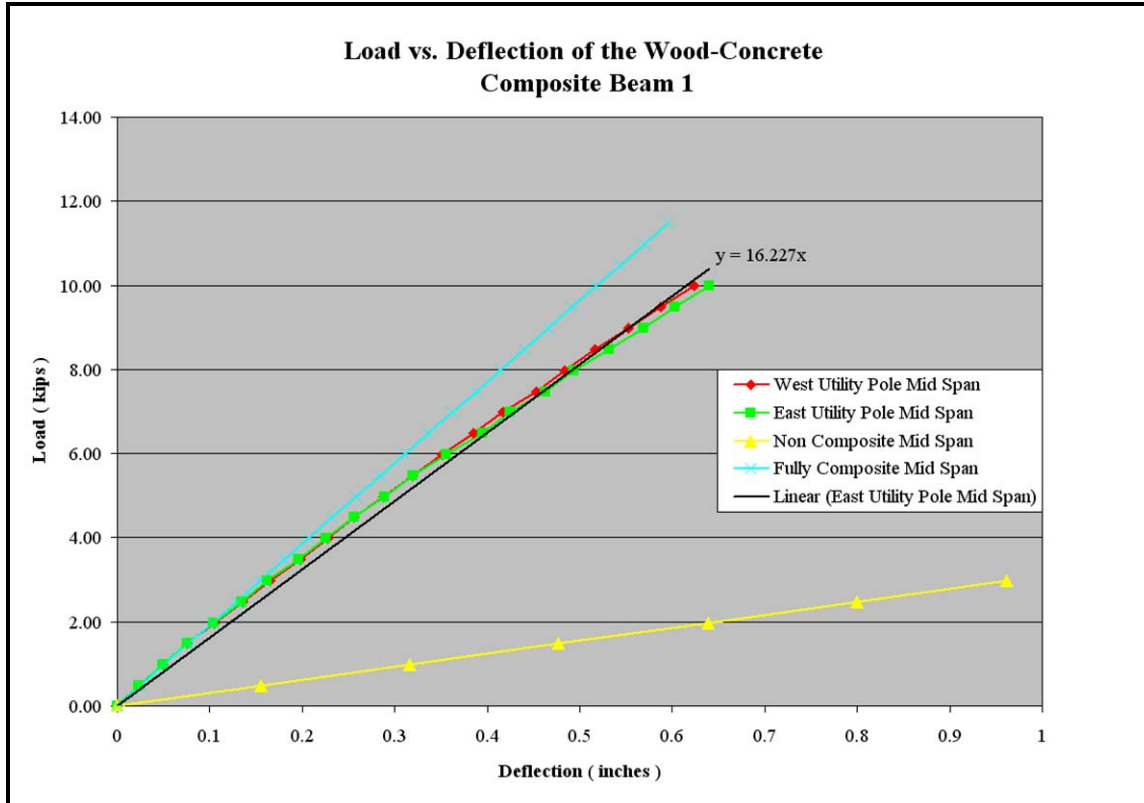


**Figure 5.11** Load vs. Deflection Plot Below the Service Load – Beam 1

Similarly, the efficiency of Wood-Concrete Composite Beam 2 in the service load range is obtained by calculating the partially composite deflection at a service load of 12.22 kips (see Figure 5.12). The slope of the trend line is used to calculate a partially composite deflection of 0.639 inches. Then the non-composite deflection at 12.22 kips is determined to be 2.555 inches and the fully composite deflection is determined to be 0.507 inches. Substituting these values into Eq. 5.12 yields:

$$EFF_{s_2} = \frac{\Delta_N - \Delta_P}{\Delta_N - \Delta_C} \rightarrow EFF_{s_2} = \frac{2.555 - 0.639}{2.555 - 0.507} \rightarrow EFF_{s_2} = 93.6\%$$

The efficiency calculations for the two beams under service loads show that the Hilti dowel and shear key connection creates a partially composite wood-concrete beam that has flexural stresses and a stiffness very close to an idealized fully composite wood-concrete beam. Yet, not accounting for the increased flexural stress due to partial composite action would make the design method presented by LeBorgne not conservative. To account for the increased flexural stress due to the partially composite action, a reduction factor designated as  $\psi$  can be employed.

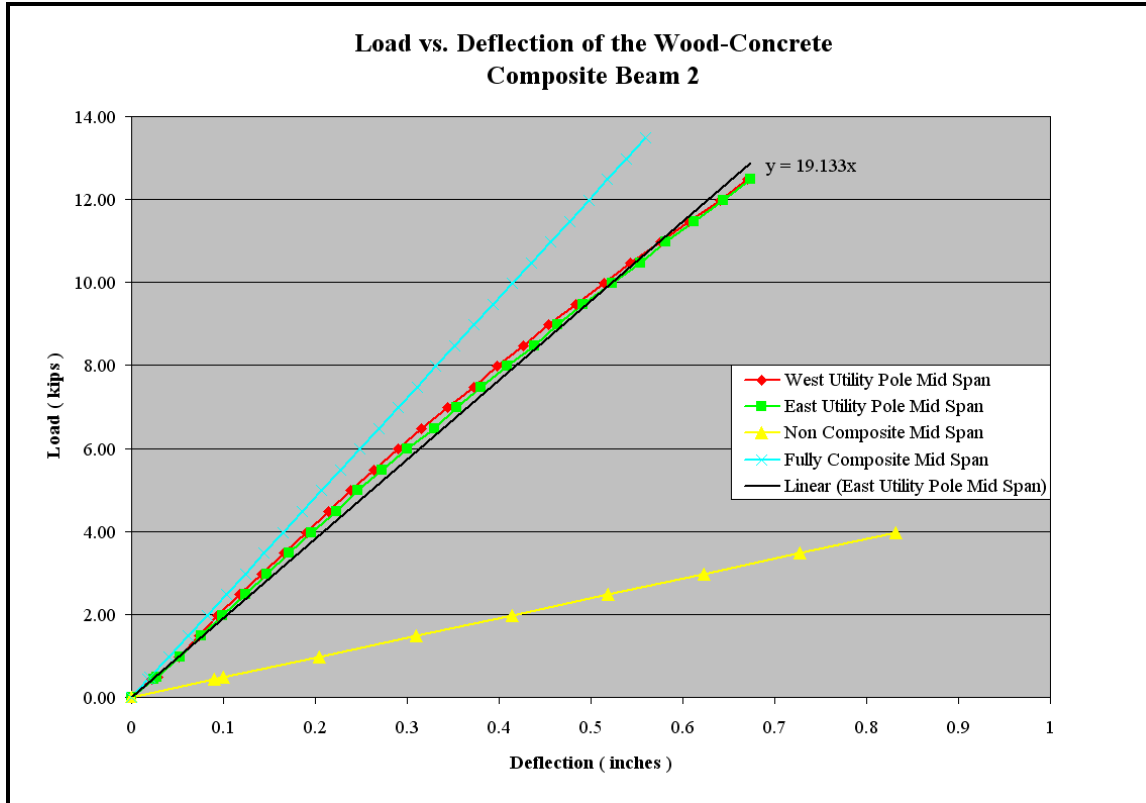


**Figure 5.12** Load vs. Deflection Plot Below the Service Load – Beam 2

The value of  $\psi$  can be found by analyzing the partially composite stresses of the wood-concrete beam through the use of Annex B in Eurocode 5<sup>20</sup>. The procedure in Annex B accounts for increased flexural stresses in the partially composite wood-concrete beam by assuming that the Hilti dowel and shear key is not a rigid connection, but instead has a flexibility equal to  $K$ . Ceccotti et al.<sup>21</sup> presented this method of using Annex B to calibrate a connection stiffness based on the actual load versus deflection data for the beam. Using the connection stiffness, the partially composite stresses can be found due to the maximum mid span moment. The moment due to the beam's dead load is subtracted from the maximum mid span moment, and the maximum factored live load from a point load at mid span can be determined. Tables 5.4 and 5.5 list the results of the extensive calculations for Wood-Concrete Composite Beams 1 and 2, respectively.

**Table 5.4** Moment and Load Comparison – Wood-Concrete Composite Beam 1

	Maximum Moment	Maximum Factored Live Load
	$M_{max}$	$P_u$
Fully Composite	1738 kip-in	15.55 kips
Partially Composite	1651 kip-in	14.58 kips
Ratio Partially/Fully	95.04 %	93.74 %

**Table 5.5** Moment and Load Comparison – Wood-Concrete Composite Beam 2

	Maximum Moment	Maximum Factored Live Load
	$M_{max}$	$P_u$
Fully Composite	2083 kip-in	19.55 kips
Partially Composite	1934 kip-in	17.86 kips
Ratio Partially/Fully	92.84 %	91.38 %

Table 5.4 shows that Wood-Concrete Composite Beam 1 had a 4.96% reduction in the allowable mid span moment by accounting for the increased flexural stresses due to the partially composite action of the wood-concrete beam. Similarly, for Wood-Concrete Composite Beam 2, there was a 7.16% reduction in mid span moment as shown in Table 6.5.

The ratios of the partially composite to fully composite maximum moment shown in Tables 5.4 and 5.5 can be used to determine the moment reduction factor,  $\psi$ . This factor is then multiplied by the fully composite mid span moment to create a reduced “partially composite” moment. The designer can choose the value of  $\psi$  based on experience. However, based on the tests performed in this research,  $\psi$  of 0.9 is a reasonable value. The value of  $\psi$  is used to reduce the maximum allowable mid span moment, as shown in the following example, to calculate the ultimate load for a beam in three point bending:

$$P_{u\_partial} = \frac{(\psi \cdot M_{max} - M_D) \cdot 4}{L} \quad \psi = 1.0 \text{ to } 0.8$$

Where  $P_{u\_partial}$  is the maximum partially composite point load applied at mid span,  $\psi$  is the moment reduction factor,  $M_{max}$  is the maximum allowable mid span moment within the beam,  $M_D$  is the moment caused by the dead load of the beam, and  $L$  is the span of the beam.

## 6. SUMMARY AND CONCLUSION

A wood-concrete composite bridge constructed of recycled utility poles is a potentially cost effective solution to repair a portion of the 108,647 rural bridges with a span less than 30 feet that have been deemed functionally obsolete or structurally deficient. Wood-concrete bridges have been in use since 1929 with an excellent record for performance and durability, with some bridges providing up to 69 years of service. As the earth's natural resources continue to become increasingly strained, designers increasingly look toward a bridge system that efficiently utilizes available materials and can be easily recycled at the end of its service life. A wood-concrete composite bridge is easily installed, requiring a minimum of materials, labor, and heavy equipment.

There are three main types of composite systems used in wood-concrete construction. The first is a non-composite system where the concrete and wood both have their own distinct neutral axes and there is no horizontal shear stress transfer between the wood and concrete layer. The second system is a partially composite system where the concrete and wood both have their own distinct neutral axes, yet since there is some horizontal shear stress across the wood-concrete layer, the neutral axes shift closer together toward the wood-concrete interface. The final system is fully composite where there is full horizontal shear transfer between the wood-concrete layers effectively bonding the wood to the concrete. Many types of connectors have been examined by various researchers to determine how to most effectively transfer horizontal shear from the wood to the concrete. In theory, if constructed well, the Hilti dowel and shear key should exhibit high efficiency as shown by Dias<sup>22</sup>. The work described herein is a confirmation of that assessment.

The ultimate goal of the research is to develop a short span deck bridge comprised of wood and concrete, where the wood utility poles serve as the wood layer. However, this research project focused on developing a design method for predicting the capacity of a section of the bridge consisting of two utility poles using the provisions of the National Design Specification, American Concrete Institute, and the American Institute of Steel Construction. Future researchers can then use this data to extend these studies to a plate model of the complete bridge deck and perform load tests on rationally configured full-width deck specimens.

Full-scale wood-concrete composite beams were constructed using recycled utility poles. The beams were sized using the design method presented by LeBorgne<sup>19</sup> with a span of 29.52 feet. Before the shear keys were cut into the beam and the concrete placed atop the wood utility poles, the modulus of elasticity for each utility pole used in the wood-concrete composite beams was determined. Then the notches were cut in the wood for the shear keys and Hilti dowels and forms were placed around the perimeter of the beam. The concrete was placed in the forms and allowed to cure for 28 days. During the 28-day curing period, the deflection of the beam was monitored versus time. At the end of the 28-day curing period, the beams were tested to failure by applying a point load at the mid span of the beam. It was found that Wood-Concrete Composite Beam 1 had an ultimate load capacity of 35.48 kips and that Wood-Concrete Composite Beam 2 had an ultimate load capacity of 37.98 kips.

The time-dependent behavior of the two wood-concrete composite beams over the 28-day curing period was analyzed to determine if it was possible to predict the mid span deflection due to the creep of the wood-concrete beam using an empirical equation and mechanics. It was deduced that if the creep was treated as a simulated uniform load acting over the length of the simply supported beam and allowed to vary in magnitude with time it would emulate the observed deflection of the beam over its 28-day curing period. The highest error between the predicted and actual deflection of the beam was 11.5% during the first six days. However, beyond this initial period, the error between the predicted and actual deflection of the beam fell below 3.5%, which corresponds to a deflection 1/16th of an inch.

As a comparison to the wood-concrete beam test data, the theoretical ultimate capacity of the wood-concrete composite beam was calculated based on whether the utility poles used in the beam's construction had material properties based on a 5% exclusion limit and mean clear wood stress corrected for defects. Both of the wood-concrete composite beams tested had ultimate failure loads consistent with if the beam was constructed of clear wood and adjusted for the actual defects in the beam, such as knots and spiral grain.

The efficiency of Wood-Concrete Beams 1 and 2 were 96.4% and 93.6%, respectively. These efficiencies are high, yet even at 93.6% efficiency there are increased flexural stresses at mid span due to partially composite action of the wood-concrete composite beam. To avoid exceeding the adjusted stress limits presented in the NDS, the maximum mid span moment needed to be reduced. The required moment reduction can be calculated by considering partially composite action using Annex B of the Eurocode. A connection stiffness based on the actual load versus deflection data for the beam was determined. Then, using the connection stiffness, the partially composite stresses were found due to the maximum mid span moment. It was found that there was a maximum 7.16% reduction in the allowable mid span moment by accounting for the increased flexural stresses due to the partially composite action of the wood-concrete beam. Another way to quantify this amount is that the partially composite moment is 92.84% of the fully composite moment. Therefore, a moment reduction factor of 0.9 multiplied by the mid span moment capacity is conservative.

## 7.1 Recommendations

The two wood-concrete composite beam specimens constructed of utility poles performed well in the ultimate load tests using ramp loading. However, when Wood-Concrete Composite Beam 1 was loaded to 1.7 times its factored design load capacity and then unloaded, there was a 0.566 inch deflection with no applied load. The concern is that cyclic loads at service capacity will generate a continuous loss in the stiffness of the wood-concrete composite beam. A vehicle traveling at highway speeds (55 mph = 80.66 ft/s) will cross a bridge with a 30-foot span in 0.37 seconds. Assuming the expected service life of a typical bridge is 50 years and a rural bridge has traffic of 100 vehicles per day, the number of load cycles a bridge experiences over its lifetime is 1,830,000. The stiffness and strength of the bridge at the end of these cycles would be useful in determining how the wood-concrete behaves over a long period of repeated load.

To apply a plate model to the results of these tests, it would be helpful to know the stiffness of the wood-concrete composite beams in torsion at mid span. The stiffness of the beam in torsion could be useful since as the deck deflects, it will most likely have a tendency to twist the utility poles and concrete deck.

Painting the entire beam worked well to prevent the wood from absorbing moisture in the fresh concrete during the curing process. One disadvantage of using a traditional waterproofing paint is that the natural beauty of the wood is masked by the white paint. It would be informative to test other types of moisture barriers such as a clear varnish. On the other hand, it should be determined if it is actually necessary to paint the entire log with a sealer.

It would be beneficial to build a full size longitudinal wood-concrete deck bridge using utility poles and instrument the base of the deck to determine the field behavior of the system under loads. Based on the data gathered from the full scale testing, a plate model could be developed for the deck or a design method adapted from one of two-way slab analysis methods presented in the ACI concrete building code.<sup>23</sup>



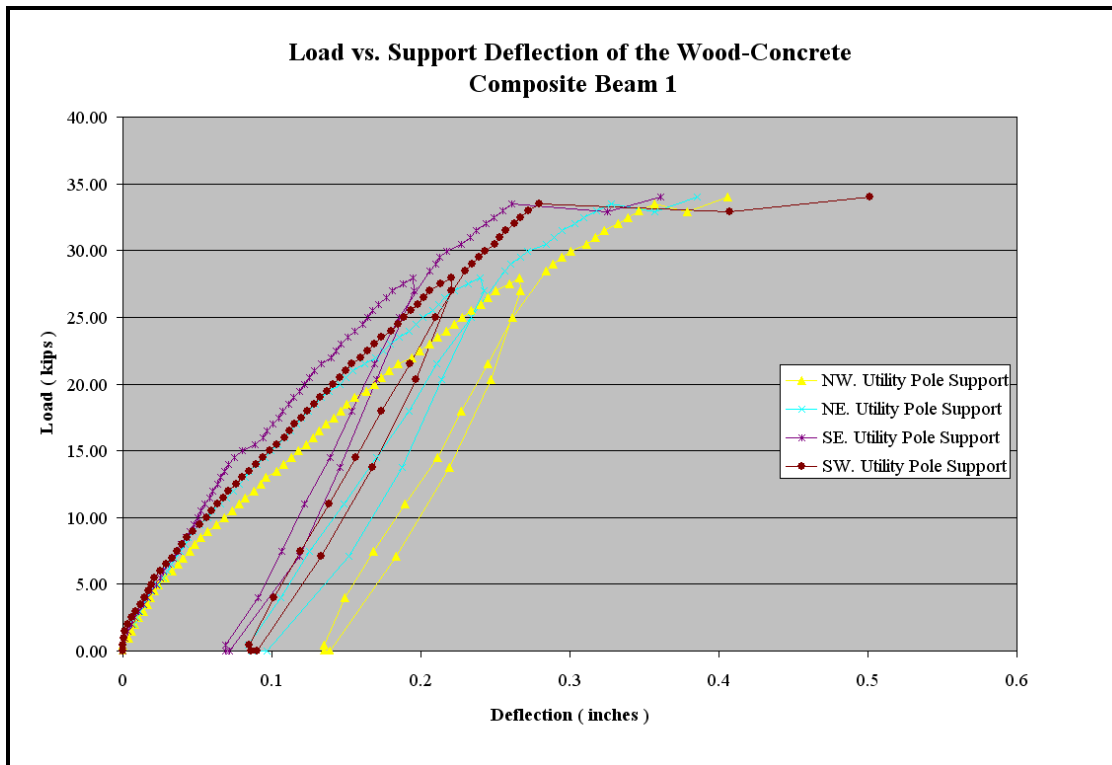
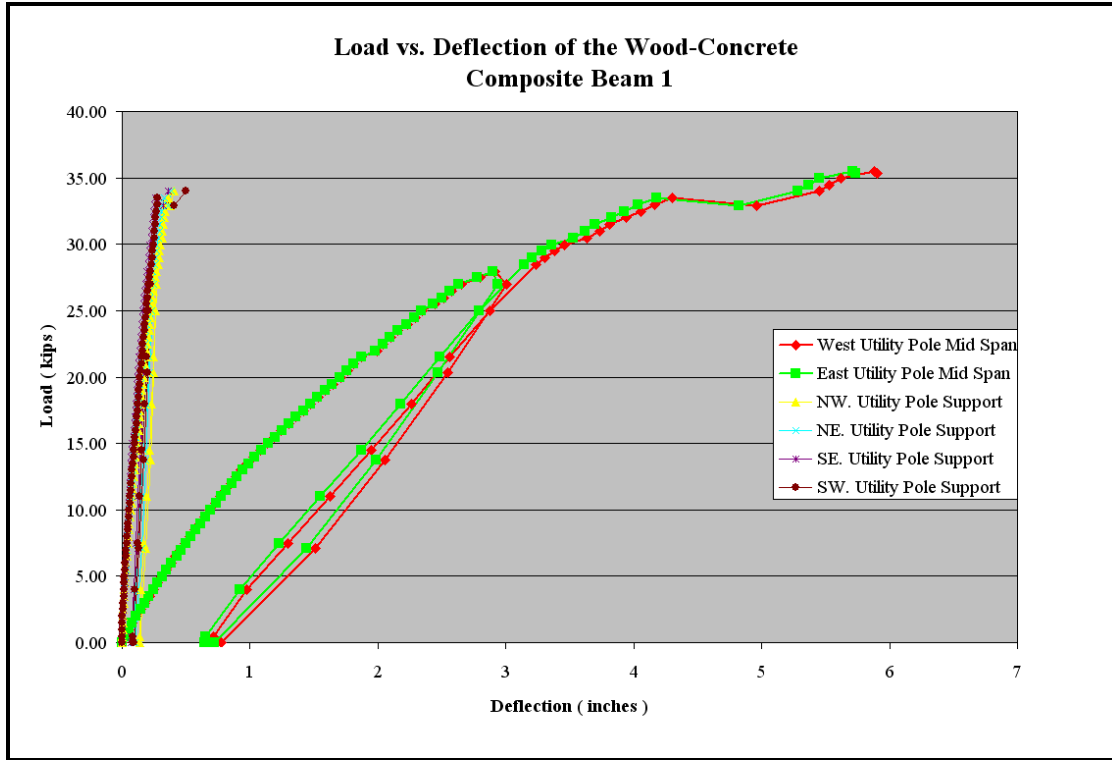
## 6. REFERENCES

1. United States. Department of Transportation, Federal Highway Administration, Office of Bridge Technology. National Bridge Inventory Database: Highway Bridge by Owner. 2006. 13 June 2007 <<http://www.fhwa.dot.gov/bridge/britab.htm>>.
2. United States. Department of Transportation, Federal Highway Administration, Office of Bridge Technology. National Bridge Inventory Database: Count of Bridges by Highway System. 2006. 13 June 2007 <<http://www.fhwa.dot.gov/bridge/britab.htm>>.
3. United States. Department of Transportation, Federal Highway Administration, Office of Bridge Technology. National Bridge Inventory Database: Count, Area, Length of Bridges by Highway System. 2006. 13 June 2007 <<http://www.fhwa.dot.gov/bridge/fc.htm>>.
4. Task Committee on Classic Wood Structures. "Classic Wood Structures." American Society of Civil Engineers (1989).
5. Lichtenstein Consulting Engineers, Inc. Delaware's Historic Bridges 2nd Edition, 2000.
6. Musser, Kevin. The History of the Three Bridges to Span the Canal Between Houghton and Hancock. 1997 <<http://www.pasty.com/copperrange/spans.htm>>.
7. McCollough, C.B. "Highway Viaducts in Oregon of Prefabricated Timber." Wood Preserving News. XII (1934): 11.
8. Baldcock, R.H., and C.B. McCollough. "Loading Tests on a New Composite Type Short Span Highway Bridge Combining Concrete and Timber in Flexure." Technical Bulletin, Oregon State Highway Department 1 (1941).
9. Pincus, G. "Behaviour of Wood-Concrete Composite Beams." American Society of Civil Engineers 39 (1970): 2009-2019.
10. Murthy, C.K. "Timber-Concrete Composites for Low Cost Housing." Housing Science Vol 8 No. 2 (1984): 209-215.
11. Pault, Jerrold. "Composite Action in Glulam Timber Bridge Systems." M.S. Thesis. Colorado State University, 1977.
12. Natterer, J., Hamm, and P. Favre. "Composite Wood-Concrete Floors for Multi-Story Buildings." Proceedings of the International Wood Engineering Conference, New Orleans, Louisiana 3 (1996): 3.431-3.435.
13. Brown, Kevin. "Testing of a Shear Key/Anchor in Layered Wood/Concrete Beams." M.S. Thesis. Colorado State University, 1998.
14. M.R. LeBorgne and R.M. Gutkowski. Provisionally Accepted, Effects of Admixtures and Shear Keys in Wood-Concrete Composite Beams, Construction and Building MATERIALS, Elsevier, Ltd, Edinburgh, Scotland.
15. Taylor, Robert. Designing with LRFD for Wood. American Wood Council. July 2001. 26 August 2007 <<http://www.awc.org/technical/LRFDStrucEng.pdf>>.

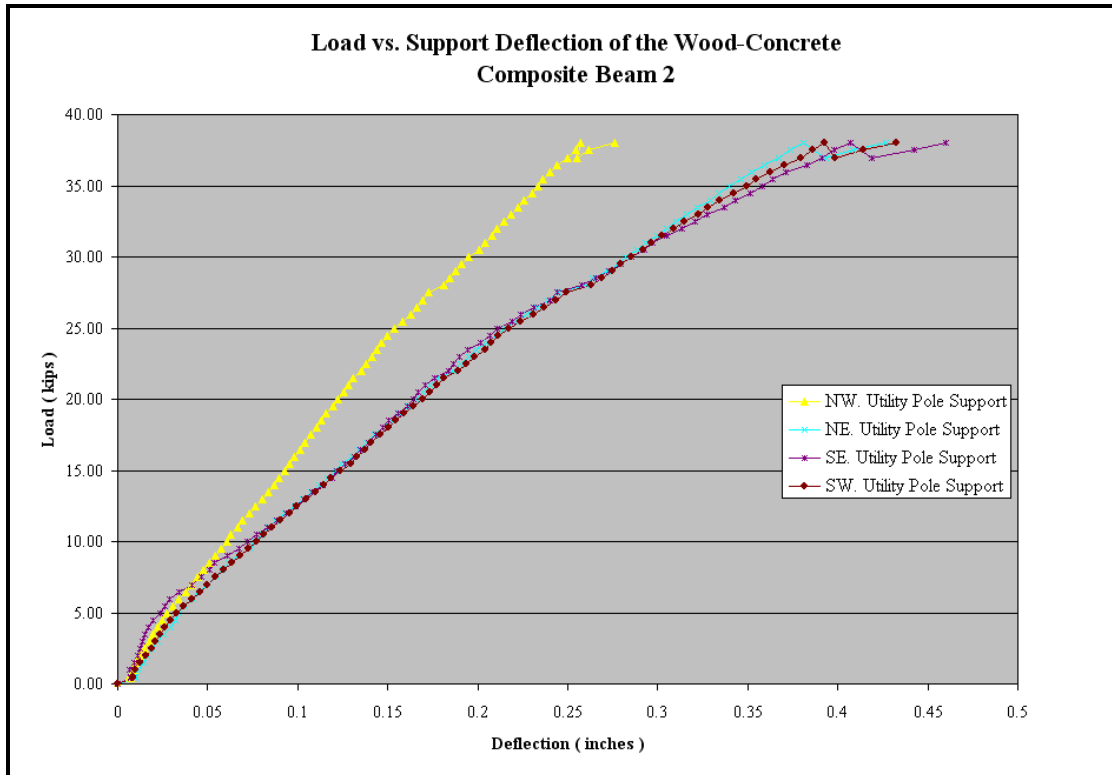
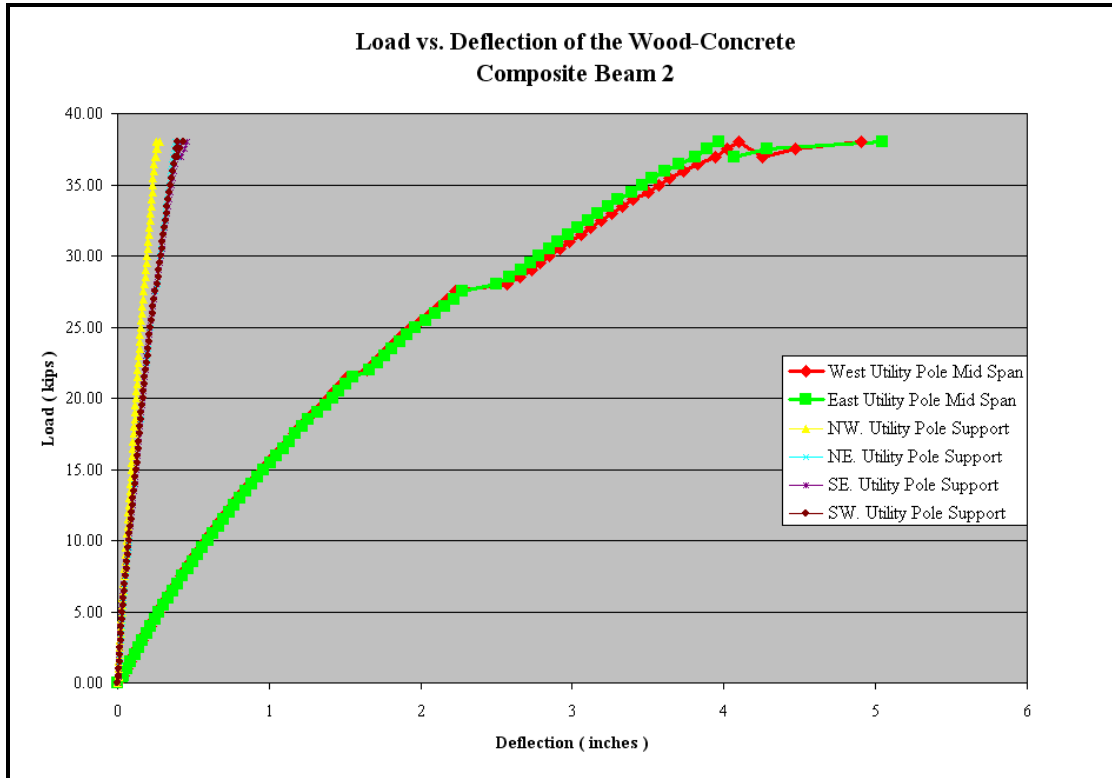
16. "ASTM D2915-03 Standard Practice for Evaluating Allowable Properties for Grades of Structural Lumber." American Standards for Testing and Materials. Vol 04.10. 2007.
17. "ASTM D245-06 Standard Practice for Establishing Structural Grades and Related Allowable Properties for Visually Graded Lumber." American Standards for Testing and Materials. Vol 04.10. 2007.
18. "ASTM D2555-06 Standard Practice for Establishing Clear Wood Strength Values." American Standards for Testing and Materials. Vol 04.10. 2007.
19. LeBorgne, Matthew. "Analysis of Wood-Concrete Beams Incorporating Recycled Utility Poles." M.S. Thesis. Colorado State University, 2007.
20. European Committee for Standardization. Eurocode 5 - Design of timber structures Part 1-1: General - Common rules and rules for buildings. prEN 1995-1-1. 2003.
21. Ceccotti, Ario, Massimo Fragiaco, Richard M. Gutkowski. On the Design of Timber-Concrete Composite Beams According to the New Versions of Eurocode 5, Proceedings, CIB-W18, International Council for Research and Innovation in Building and Construction, Working Commission W18- Timber Structures, Meeting Thirty-Five, Kyoto, Japan, September 2002.
22. Dias A.M. P.G.. "Mechanical behaviour of timber-concrete joints." Ph.D. Thesis, Univ. of Coimbra, Coimbra, Portugal. 2005.
23. American Concrete Institute. 318-05: Building Code Requirements for Structural Concrete and Commentary. 2005.

# APPENDIX A. SUPPORT DEFLECTION

## WOOD-CONCRETE BEAM 1



## WOOD-CONCRETE BEAM 2



- 
- 1 United States. Department of Transportation, Federal Highway Administration, Office of Bridge Technology. National Bridge Inventory Database: Highway Bridge by Owner. 2006. 13 June 2007 <<http://www.fhwa.dot.gov/bridge/britab.htm>>.
  - 2 United States. Department of Transportation, Federal Highway Administration, Office of Bridge Technology. National Bridge Inventory Database: Count of Bridges by Highway System. 2006. 13 June 2007 <<http://www.fhwa.dot.gov/bridge/britab.htm>>.
  - 3 United States. Department of Transportation, Federal Highway Administration, Office of Bridge Technology. National Bridge Inventory Database: Count, Area, Length of Bridges by Highway System. 2006. 13 June 2007 <<http://www.fhwa.dot.gov/bridge/fc.htm>>.
  - 4 Task Committee on Classic Wood Structures. "Classic Wood Structures." American Society of Civil Engineers (1989).
  - 5 Lichtenstein Consulting Engineers, Inc. Delaware's Historic Bridges 2nd Edition, 2000.
  - 6 Musser, Kevin. The History of the Three Bridges to Span the Canal Between Houghton and Hancock. 1997 <<http://www.pasty.com/copperrange/spans.htm>>.
  - 7 McCollough, C.B. "Highway Viaducts in Oregon of Prefabricated Timber." Wood Preserving News. XII (1934): 11.
  - 8 Baldcock, R.H., and C.B. McCollough. "Loading Tests on a New Composite Type Short Span Highway Bridge Combining Concrete and Timber in Flexure." Technical Bulletin, Oregon State Highway Department 1 (1941).
  - 9 Pincus, G. "Behaviour of Wood-Concrete Composite Beams." American Society of Civil Engineers 39 (1970): 2009-2019
  - 10 Murthy, C.K. "Timber-Concrete Composites for Low Cost Housing." Housing Science Vol 8 No. 2 (1984): 209-215.
  - 11 Pault, Jerrold. "Composite Action in Glulam Timber Bridge Systems." M.S. Thesis. Colorado State University, 1977.
  - 12 Natterer, J., Hamm, and P. Favre. "Composite Wood-Concrete Floors for Multi-Story Buildings." Proceedings of the International Wood Engineering Conference, New Orleans, Louisiana 3 (1996): 3.431-3.435.
  - 13 Brown, Kevin. "Testing of a Shear Key/Anchor in Layered Wood/Concrete Beams." M.S. Thesis. Colorado State University, 1998.
  - 14 M.R. LeBorgne and R.M. Gutkowski. Provisionally Accepted, Effects of Admixtures and Shear Keys in Wood-Concrete Composite Beams, Construction and Building MATERIALS, Elsevier, Ltd, Edinburgh, Scotland.
  - 15 Taylor, Robert. Designing with LRFD for Wood. American Wood Council. July 2001. 26 August 2007 <<http://www.awc.org/technical/LRFDStrucEng.pdf>>.
  - 16 "ASTM D2915-03 Standard Practice for Evaluating Allowable Properties for Grades of Structural Lumber." American Standards for Testing and Materials. Vol 04.10. 2007.
  - 17 "ASTM D245-06 Standard Practice for Establishing Structural Grades and Related Allowable Properties for Visually Graded Lumber." American Standards for Testing and Materials. Vol 04.10. 2007.
  - 18 "ASTM D2555-06 Standard Practice for Establishing Clear Wood Strength Values." American Standards for Testing and Materials. Vol 04.10. 2007.
  - 19 LeBorgne, Matthew. "Analysis of Wood-Concrete Beams Incorporating Recycled Utility Poles." M.S. Thesis. Colorado State University, 2007.

---

20 European Committee for Standardization. Eurocode 5 - Design of timber structures Part 1-1: General - Common rules and rules for buildings. prEN 1995-1-1. 2003.

21 Ceccotti, Ario, Massimo Fragiaco, Richard M. Gutkowski. On the Design of Timber-Concrete Composite Beams According to the New Versions of Eurocode 5, Proceedings, CIB-W18, International Council for Research and Innovation in Building and Construction, Working Commission W18- Timber Structures, Meeting Thirty-Five, Kyoto, Japan, September 2002.

22 Dias A.M. P.G.. "Mechanical behaviour of timber-concrete joints." Ph.D. Thesis, Univ. of Coimbra, Coimbra, Portugal. 2005.

23. American Concrete Institute. 318-05: Building Code Requirements for Structural Concrete and Commentary. 2005.